Immune modulatory effects of lapatinib and erlotinib on EGFR-associated pathways in head and neck squamous cell carcinoma

Dissertation

zur Erlangung des

Doktor der Medizin (Dr. med.)

vorgelegt

der Medizinischen Fakultät

der Martin-Luther-Universität Halle-Wittenberg

vorgelegt von

Herrn Bo Yang

Betreuer/Betreuerin: Prof. Dr. Barbara Seliger

Prof. Dr. Claudia Wickenhauser

Gutachter: Prof. Dr. Rüdiger Horstkorte, Halle (Saale)

Prof. Dr. Michael Bachmann, Dresden

Datum der Verteidigung: 06.12.2023

I dedicate this thesis to my beloved wife, Qiuhui Yao, and my dear son, Zhiyuan Yang.

Abstract

The treatment of patients with head and neck squamous cell carcinoma (HNSCC) is extraordinarily complex and challenging, and despite the availability of novel targeted drugs and immunotherapies, the mortality rate of HNSCC patients has not decreased significantly over the past decades. The activation of the epidermal growth factor receptor (EGFR) and transforming growth factor β (TGFβ) signaling pathways play a role in the neoplastic transformation of HNSCC and negatively influence immune responses, which has been linked to the initiation and progression of the disease. The efficiency of immunotherapeutic strategies, such as immune checkpoint inhibitors (ICPI), often depend on the expression of major histocompatibility complex class I (MHC-I) and programmed cell death ligand-1 (PD-L1). The EGFR inhibitors lapatinib and erlotinib are known to impede the development of tumors; however, the effect of the inhibitors on the immunogenicity of HNSCC has not yet been investigated in detail. Therefore, the aim of the study was to determine (i) whether inhibitors of the EGFR pathway influence the expression of immune stimulatory/ immune inhibitory and immune response relevant molecules and (ii) whether the expression of signal transduction molecules modulate the immunogenicity of HNSCC lesions, the immune infiltration as well as the patient's survival. Both EGFR inhibitors effectively enhance human leukocyte antigen A, B and C (HLA-ABC) expression, while reducing PD-L1 expression in HNSCC cell lines. In some HNSCC cells, the treatment with EGFR inhibitors significantly decreased the EGFR phosphorylation and its downstream protein kinase B (PKB; also known as AKT) and extracellular signal-regulated kinase (ERK). In response to EGFR inhibitor treatment, the mRNA levels of TGFβ family members and their receptors were variably elevated in the group of primary and metastatic tumor cell lines, which may explain the activation of AKT and ERK. Moreover, tyrosine kinase inhibitor (TKI) treatment of HNSCC modulates the expression of chemokines and the immune cell infiltration in tissue samples from patients with HNSCC. The altered expression of HLA-ABC and PD-L1 indicated that the combination of the TKI with immunotherapy might significantly improve the outcome of HNSCC patients.

Bo, Yang: **Immune modulatory effects of lapatinib and erlotinib on EGFR-associated pathways in head and neck squamous cell carcinoma**, Halle, Univ., Med. Fak., Diss., pages – 64, figures – 18, tables – 4, 2023.

Referat

Die Behandlung von Patienten mit Kopf-Hals-Plattenepithelkarzinomen (HNSCC) ist außerordentlich komplex und herausfordernd und trotz der Verfügbarkeit neuartiger zielgerichteter Medikamente und Immuntherapien ist die Sterblichkeitsrate von HNSCC-Patienten in den letzten Jahrzehnten nicht wesentlich gesunken. Die Aktivierung der Signalwege des epidermalen Wachstumsfaktorrezeptors (EGFR) und des transformierenden Wachstumsfaktors-β (TGF-β) von HNSCC spielt eine Rolle bei der neoplastischen Transformation und geht mit einer verminderten Immunreaktion einher, die mit der Initiation und dem Fortschreiten der Krankheit in Verbindung gebracht werden. Die Wirksamkeit immuntherapeutischer Strategien, wie Immuncheckpunkt-Inhibitoren (ICPI) hängt häufig von der Expression des Haupthistokompatibilitätskomplexes Klasse-I (MHC-I) und des programmierten Zelltod-Liganden-1 (PD-L1) ab. Die EGFR-Inhibitoren Lapatinib und Erlotinib sind dafür bekannt, dass sie das Tumorwachstum hemmen; die Auswirkungen dieser Inhibitoren auf die Immunogenität von HNSCC wurden jedoch bisher kaum untersucht. Ziel der Studie war es daher festzustellen, ob (i) Inhibitoren des EGFR-Signalwegs die Expression immunstimulierender/ inhibierender und für die Immunantwort relevanter Moleküle beeinflussen und (ii) ob die Expression von Signaltransduktionsmolekülen die Immunogenität von HNSCC-Läsionen, die Immuninfiltration sowie das Überleben der Patienten moduliert. Beide EGFR-Inhibitoren verstärken die Expression der humanen Leukozytenantigene A, B und C (HLA-ABC), während sie die PD-L1-Expression in HNSCC-Zelllinien reduzieren. In einigen HNSCC-Zellen führte die Behandlung mit EGFR-Inhibitoren zu einer deutlichen Verringerung der EGFR-Phosphorylierung und der nachgeschalteten Proteinkinase B (PKB; auch als AKT bekannt) und der extrazellulären signalregulierten Kinase (ERK). Als Reaktion auf die Behandlung mit EGFR-Inhibitoren waren die mRNA-Spiegel der Mitglieder der TGF-β-Familie und ihrer Rezeptoren in der Gruppe der primären und metastatischen Tumorzelllinien unterschiedlich stark erhöht, was die Aktivierung von AKT und ERK erklären könnte. Darüber hinaus moduliert die Behandlung von HNSCC mit Tyrosinkinaseinhibitoren (TKI) die Expression von Chemokinen und die Infiltration von Immunzellen in Gewebeproben von Patienten mit HNSCC. Die veränderte Expression von HLA-ABC und PD-L1 deutet darauf hin, dass eine Kombination von beiden TKI mit Immuntherapie die Ergebnisse von HNSCC-Patienten deutlich verbessern könnte.

Bo, Yang: **Immunmodulierende Effekte von Lapatinib und Erlotinib auf EGFR-assoziierte Signalwege bei Plattenepithelkarzinomen des Kopfes und Halses**, Halle, Univ., Med. Fak., Diss., Seiten – 64, Abbildungen – 18, Tabellen – 4, 2023.

Contents:

Abbreviations

Abbreviation	Meaning
2D	Two-dimensional
3D	Three-dimensional
Ab	Antibody
ADC	Antibody–drug conjugate
AKT	Protein kinase B
ALAS1	Delta-aminolevulinate synthase 1
APM	Antigen processing machinery
ATP	Adenosine triphosphate
B cell	B lymphocyte
BSA	Bovine serum albumin
CTL	Cytotoxic T lymphocyte
CTLA-4	Cytotoxic T lymphocyte-associated protein 4
DC	Dendritic cell
ddH2O	Double-distilled water
DMSO	Dimethyl sulfoxide
EBV	Epstein-Barr virus
EDTA	Ethylene diamine tetraacetic acid
EGFR	Epidermal growth factor receptor
ERK	Extracellular signal-regulated kinase
FACS	FACS fluorescence-activated cell-sorting
FDA	Food and Drug Administration
FOXP3	Forkhead box protein P3
HC	Heavy chain
ERBB2	Human epidermal growth factor receptor 2
HLA	Human leukocyte antigen
HNC	Head and neck cancer
HNSCC	Head and neck squamous cell carcinoma
HPV	Human papillomavirus

IC50	Half-maximal inhibitory concentration
ICP	Immune checkpoint
ICPI	Immune checkpoint inhibitor
IFN	Interferon
JNK	c-Jun N-terminal kinase
mAb	Monoclonal antibody
MAPK	Mitogen-activated protein kinase
MDSC	Myeloid-derived suppressor cell
MHC-I	Major histocompatibility complex class I
mTOR	Mammalian target of rapamycin
NK cell	Natural killer cell
NSCLC	Non-small cell lung cancer
OS	Overall survival
OSCC	Oropharyngeal squamous cell carcinoma
p-AKT	Phospho-Akt
p-EGFR	Phospho-EGFR, phospho-HER1
p-ERK	Phospho-ERK
PBMC	Peripheral blood mononuclear cell
PBS	Phosphate-buffered saline
PCR	Polymerase chain reaction
PD-1	Programmed cell death protein 1
PD-L1	Programmed cell death 1 ligand 1
PE	Phycoerythrin
PI3K	Phosphoinositide 3-kinase
PTK	Protein tyrosine kinase
RCC	Renal cell carcinoma
RT-PCR	Real-time PCR
STAT1	Signal transducer and activator of transcription 1
T cell	T lymphocyte
T reg cell	Regulatory T cell

TAM	Tumor-associated macrophage
TAP	Transporter associated with antigen processing
TCGA	The Cancer Genome Atlas
TCR	T cell receptor
TGFβ	Transforming growth factor-beta
TGFβR	Transforming growth factor beta receptor
Th1	T helper 1
TIL	Tumor immune infiltrating cell
TIL-B	Tumor infiltrating B cell
TKI	Tyrosine kinase inhibitor
Tm	Melting temperature
TME	Tumor microenvironment
Treg	Regulatory T cell
Tris	Tris (hydroxymethyl) aminomethane hydrochloride
TTP	Tristetraprolin
WB	Western blot
WHO	World Health Organization
β2m	β2-microglobulin

1 Introduction

1.1 Characteristics of head and neck squamous carcinoma

Cancer is one of the leading causes of death worldwide and a significant barrier of increasing life expectancy [1]. It is the third or fourth major cause of death before the age of 70 in 23 countries, and the first or second leading cause in 112 of 183 nations. According to estimates from the World Health Organization (WHO) in 2019, head and neck cancers (HNCs) are the seventh most prevalent type of cancer worldwide and refer to a variety of malignant tumors that arise from different anatomical sites that comprise the upper respiratory tract, including the lips, mouth, nasopharynx, oropharynx, hypopharynx, larynx, and salivary glands. Among these cancers, squamous cell carcinoma of the head and neck (HNSCC) accounts for more than 90% of HNCs [2]. Longstanding evidence links tobacco use to HNSCC and is a major risk factor with increasing prevalence in developing nations [3]. Chronic heavy alcohol consumption is another independent risk factor for HNCs, particularly for HNSCC [4], which also enhances the carcinogenic effects of tobacco. In addition, the increased prevalence of human papillomavirus (HPV) infection is associated with an increased incidence of oropharyngeal cancer [5]. Of the 120 different HPV types that have been identified, the oncogenic type 16 (associated with the majority of cases) and oncogenic type 18 of HPV account for more than 90% of HPV-associated oropharyngeal squamous cell carcinoma (OSCC) cases [6]. Oral sexual activity is a major risk factor of HPV infection [7]. Next to HPV, Epstein-Barr virus (EBV) infection is associated with nasopharyngeal cancer [8]. Other less studied and addressed risk factors for HNCs include genetic susceptibility [9], laryngopharyngeal reflux [10], betel nut chewing [11], marijuana [12], diets high in animal fat and low in fruits and vegetables [13], particular occupations, air pollution [14] and radiation exposure [15]. HNSCCs are currently treated with surgery, anti-cancer drug therapy and radiation. However, many patients relapse within three to five years of completing this therapy. In recent years, immune checkpoint inhibitors (ICPIs) have demonstrated significant anticancer activity in various cancers, including HNCs and improve the overall survival (OS) and quality of life in HNSCC patients compared to chemotherapy and radiotherapy [16, 17].

1.2 Immune infiltration in head and neck squamous carcinoma

The high probability of recurrence and/or metastasis in patients is a key deterrent to HNSCC treatment, which not only emphasizes the difficulties of treating HNSCCs, but also conveys their complicated immunological and molecular features. The high incidence of metastatic HNSCC and recurrence is likely attributable to the interactions between the surrounding tissue

matrix and immune cells that comprise the tumor microenvironment (TME). The host immune system is capable of identifying and destroying neoplastic cells; nevertheless, evasion of immunosurveillance provides an environment leading to tumor cell development and survival [18, 19]. It has also been demonstrated that the TME of HNSCC impairs tumor-infiltrating lymphocyte (TIL) function [20, 21]. The TME contains many subpopulations of cells, including cancer-associated stromal fibroblasts, T cells, B cells, neutrophils, macrophages, myeloid-derived suppressor cells (MDSCs), natural killer (NK) cells, and mast cells [20, 22-27]. Bioinformatics analysis of Mandal et al. demonstrated that HNSCC is both one of the most immune-infiltrated and the most NK cell– and Treg cell–infiltrated cancer type [28]. Tumor infiltrating B cells (TIL-Bs) represent a potential new target to complement T cell-based immunotherapies, as they are prevalent in many human malignancies and correlate positively with favorable patient outcomes [29, 30], TIL-Bs in HNSCC have the potential to contribute to the anti-tumor immunity in a number of ways, including the presentation of tumor antigens to $CD4^+$ T cells [31]. Liang et al. identified substantial differences between HNSC tissues and surrounding non-cancerous tissues in terms of naive B cells, monocytes, resting mast cells, active mast cells, $CD8^+$ T cells and M0 macrophages. Some subgroups of TILs were substantially linked with the clinical outcome [32]. Cancer, tissue-resident and recruited immune cells that express several chemokine ligands and receptors affect carcinogenesis [33, 34]. In many malignancies, tumor-intrinsic genetic alterations and tumorigenesis-induced extrinsic stress signals produce inflammatory cytokines and chemokines that initiate inflammation [35]. CC chemokines are essential for migration and differentiation and cellular interaction of $CD4^+$ and $CD8^+$ lymphocytes, dendritic cells (DCs), eosinophils, macrophages, monocytes, NK cells, and neoplasia [36]. Using locally produced chemotactic factors including CCL2 and CCL5, circulating monocytes become tumor-associated macrophages (TAMs) [37]. CXCL9, -10/CXCR3 regulate the immune cell motility, differentiation, and activation. This axis promotes the maturation of naive T cells into T helper 1 (Th1) cells and directs immune cell migration to their focus areas by recruiting immune cells like CTLs, NK cells, NKT cells and macrophages [38]. CCL22 is a potent chemoattractant for T lymphocytes, NK cells, monocytes and DCs exposed to antigens [39], both DCs and macrophages were the main producers of CCL22 in tumors [40], T cells and B cells can also express CCL22 following activation [41, 42].

1.3 Features of the epidermal growth factor receptor

The epidermal growth factor receptor (EGFR) family is a transmembrane glycoprotein composed of an extracellular ligand-binding domain and a cytoplasmic tyrosine kinase domain.

It is composed of four related receptor tyrosine kinases with common structural elements, including EGFR (HER1/ERBB1), ERBB2 (HER2/neu), ERBB3 (HER3), and ERBB4 (HER4) [43, 44], which are key mediators in cell signaling pathways involved in cell proliferation, apoptosis, angiogenesis, and metastatic spread [45, 46]. The ERBB tyrosine kinase family members are among the most frequently altered proteins in cancer and aberrant tyrosine kinase activation caused by gene mutations can drive tumorigenesis, tumor growth, and progression [47]. Several types of cancer, including breast, endometrial, ovarian, prostate, glioma, medulloblastoma, HNSCC, non-small cell lung cancer (NSCLC), esophageal, gastric, colon, colorectal, anal, pancreatic, bladder, and melanoma, have been associated with oncogenic alterations of genes encoding ERBB family members [48-50]. Thus, molecular-targeted therapies, such as tyrosine kinase inhibitors (TKIs), monoclonal antibodies (mAbs), and antibody–drug conjugates (ADCs), targeting oncogenic EGFR or human epidermal growth factor receptor 2 (ERBB2) signaling have been developed and successfully used in the clinic, resulting in improved survival of patients with cancers harboring these gene alterations [51-53].

1.4 Role of epidermal growth factor receptor-related pathways in cancers

As described above, EGFR, a member of the ERBB family, is a transmembrane glycoprotein with an extracellular ligand-binding domain and a cytoplasmic domain with tyrosine kinase activity involved in signal transduction. Upon ligand binding, EGFR activation initiates multiple important signaling cascades, including the RAS/RAF/MEK/ERK and PI3K/AKT/mTOR pathways [54, 55] (Figure 1), the ERK/MAPK signaling pathway. This signaling network plays a crucial role in regulating diverse cellular physiological processes, including cell growth, development, division and apoptosis. Many human malignancies, including ovarian, colon, breast, thyroid, pancreatic, brain, and lung cancers, have an elevated activation of the ERK/MAPK signaling pathway [56-58]. Activated ERK enter the nucleus and bind to transcription factors to regulate cell proliferation, differentiation, apoptosis and transcription in response to extracellular stimuli [59, 60]. *In vivo*, continuous activation of the ERK/ MAPK signaling pathway can stimulate the transformation of normal to neoplastic cells, whereas inhibition of this pathway can limit tumor growth [61]. Thus, components of the ERK signaling cascade are promising therapeutic targets for cancer therapy, and the blockade of this signaling module by specific inhibitors is a crucial antitumor approach [62]. Akt is a well-characterized effector of the phosphoinositide 3-kinase (PI3K) in the PI3K/Akt/mTOR signaling pathway and its deregulation is crucial for the development of a number of human malignancies [63].

Numerous human cancers exhibit recurrent AKT activation [64], which has been linked to disease progression and/or a poor prognosis of multiple tumor types [64] and found in 40% of breast, ovarian epithelial, prostate and gastric cancers [65, 66]. Numerous oncoproteins and tumor suppressors are intertwined in the Akt pathway leading to cell proliferation, differentiation, apoptosis inhibition as well as actin cytoskeleton rearrangement [67].

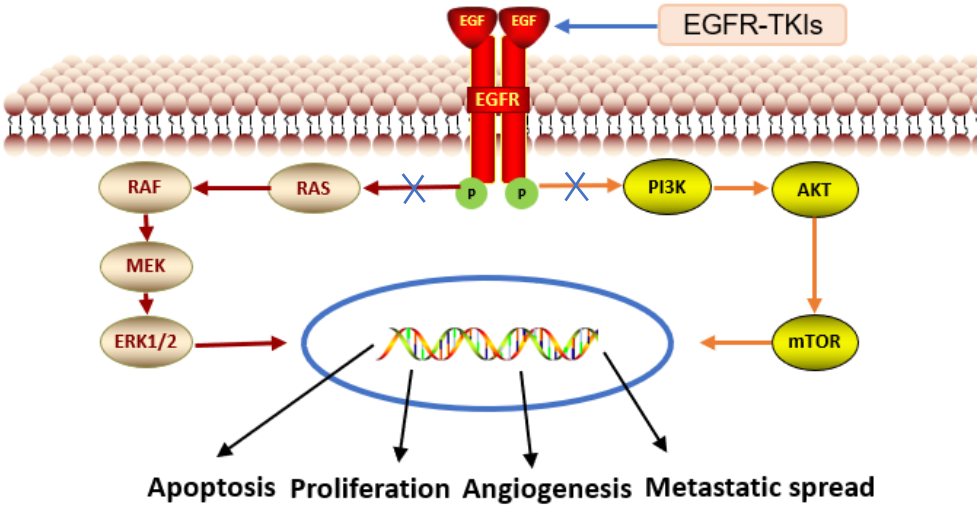

Figure 1. EGFR-related ERK and AKT pathway. EGFR-TKIs can inhibit the activation of the MAPK (RAS-RAF-MEK-ERK) and phosphatidylinositol 3-kinase (PI3K) pathway (PI3K-AKT-mTOR) signaling pathway. The figure was created using the ScienceSlides and PowerPoint software.

1.5 ERBB protein family as a target for cancer treatment

Protein tyrosine kinases (PTKs) are a class of proteins with tyrosine kinase activity that catalyze the transfer of phosphate groups on adenosine triphosphate (ATP) to the tyrosine residues of many important proteins. Upon their phosphorylation, they then transmit signals to regulate a number of physiological and biochemical processes, including cell properties, differentiation and apoptosis [68]. PTK disorders can result in a wide array of diseases within the body. More than fifty percent of proto-oncogenes and oncogene products have PTK activity and their aberrant expression can lead to disruptions in the regulation of cell proliferation and ultimately cause tumorigenesis [69]. Moreover, abnormal PTK expression is linked to tumor invasion and metastasis, tumor neovascularization and tumor (chemo)therapy resistance [70]. In anti-tumor pharmacological research, PTKs as targets for drug development have become a hot topic. Major international research institutions and pharmaceutical companies are investing heavily in developing drugs that target PTKs, such as selective TKIs that target specific molecular pathways upregulated in certain cancers [71]. Lapatinib is a reversible dual EGFR and ERBB2 inhibitor and inhibits the growth of tumor cells by binding to the ATP-binding

site of the intracellular structural domain of the receptor and inhibiting the activity of EGFR and ERBB2 tyrosine kinases [72, 73]. Lapatinib inhibits MAPK and PI3K signaling in tumor cell lines that overexpress EGFR and ERBB2 [74, 75]. The response to lapatinib was significantly correlated with ERBB2 overexpression and inhibited AKT and ERK phosphorylation. In 2007 the Food and Drug Administration (FDA) approved lapatinib for the treatment of breast, NSCLC, head and neck, and gastric cancers [76]. Erlotinib is a TKI of the first generation that targets the EGFR [77]. Numerous studies have demonstrated the anti-tumor effects of EGFR inhibitors in combination therapy for the treatment of NSCLC and squamous cell lung cancer [78]. However, these molecular targeted therapies have struggled to produce long-lasting clinical benefits, highlighting the need for more effective cancer treatments [79].

1.6 Function of transforming growth factor beta family in cancer

Numerous studies have shown that the transforming growth factor beta **(**TGFβ) signaling pathway is crucial for cell cycle regulation, influencing cell proliferation, migration, differentiation, invasion and apoptosis [80]. In addition, TGFβ is the major regulator of the immune responses by inhibiting Th1 cells, Th2 cells, $CD8^+$ cytotoxic T lymphocytes (CTLs), macrophages, NK cells, B cells and granulocytes [81]. The three canonical TGFβ signaling ligands TGFβ1, TGFβ2 and TGFβ3 initiate TGFβ signaling upon binding to the cell surface transmembrane TGFβ receptor type II (TGFβR2) [82]. The TGFβ receptor type I (TGFβR1) is recruited into a tetrameric complex with TGFβR2 upon ligand binding and TGFβR2 kinase activity initiates phosphorylation of the TGFβR1 on serine/threonine residues. The TGFβR3 binds to the cytoplasmic domain of TGFβR2 and dissociates upon recruitment of TGFβR1, thereby facilitating the formation of the TGFβR2-TGFβR1 activation signaling complex [83, 84]. TGFβ is a double-edged sword in cancer progression. In normal epithelial or premalignant cells and the early stages of tumor development [85], TGFβ frequently functions as a tumor suppressor. However, when tumor cells become resistant to the anti-mitotic effects, TGFβ can be converted into a tumor promoter [86] and advanced tumors such as breast cancer, glioma and melanoma benefit from the TGFβ/SMAD pathway [87]. TGFβ can also signal via several non-canonical (SMAD-independent) pathways, including ERK, MAP kinase, PI3K, AKT, and JNK [88-90] (Figure 2). Despite the evidence that the TGFβ family can modulate anti-tumor immune responses, its role in tumors has still to be further clarified.

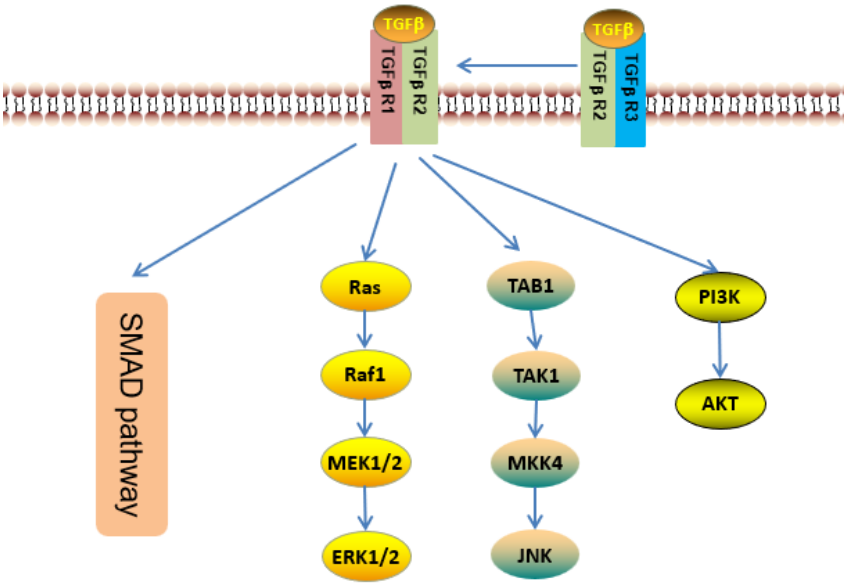

Figure 2. TGFβ signaling pathway. TGFβ ligands bind to the TGFβR leading to the activation of the TGFβ/SMAD signaling as well as a SMAD-independent activation of the TGFβ pathway involving signaling via MEK/ERK, JNK and PI3K-AKT. The figure was created using the ScienceSlides and PowerPoint software.

1.7 Relationship between cancer and immune response

Cancer is frequently characterized by genetic instability as well as various structural abnormalities that occur during tumor progression [91, 92]. These genomic variants can generate tumor antigens that the immune system recognizes as foreign, eliciting a cellular immune response [93]. The immune system plays a crucial role in immune surveillance [94, 95]. Cells of the adaptive and innate immune systems can infiltrate the tumor microenvironment (TME) and regulate tumor development [96, 97]. Innate immune cells include natural killer (NK) cells, eosinophils, basophils, mast cells, neutrophils, monocytes, macrophages and DCs, which contribute to tumor suppression by either directly killing tumor cells or triggering adaptive immune responses [98]. The adaptive immune system comprises of lymphocytes, such as B cells and T cells, with B cells playing a major role in humoral immune responses and T cells in cell-mediated immune responses [99]. Evidence accumulated over the past decade from mouse models and human cancer patients suggests that the immune system plays a crucial role in recognizing and eliminating transformed malignant cells. Moreover, depending on the immune cell sub-populations, the immune system may also promote the progression of tumors [100]. Furthermore, the abnormal expression of chemokine ligands or chemokine receptors has also been linked to dysfunctional lymphoid organ development and a deficient or exaggerated immune response, and thus might be involved in tumor progression [34].

1.8 Immune escape mechanism in cancer

Under physiological conditions, innate and adaptive immune cells can eradicate cancer cells through immunosurveillance [101]. However, cancer cells acquire the ability to escape from the anti-tumor immune response, and the deregulated relationship between antagonistic effectors and regulatory immune cells leads to a TME that can promote cancer development [102]. In order to progress, cancer avoid the immune control. It is now widely accepted that cancer cells can successfully evade immune surveillance by overexpressing self-associated molecular patterns, which can directly inhibit immune cell function by activating immune checkpoints (ICPs) or induce the differentiation of immune-suppressive cells that further reduce the activity of anti-tumoral effects cells [103]. Some mechanisms involve mutations and deletions in structural genes of one or more antigen presentation pathway components; others affect the transcription of pathway genes via loss of transcription factors or epigenetic silencing of gene regulatory elements [104]. HNSCC can avoid immune surveillance by reducing essential anti-tumor immune signaling processes resulting in tumor development [105]. Other major immune-suppressive mechanisms include the resistance of checkpoint inhibitors and reduced T cell receptor (TCR) activity. The induction of T cell death and upregulation of immunosuppressive Th2-type cytokines accelerated the recruitment of regulatory T cells (Tregs), MDSCs or M2 macrophages in the TME, while chemokines are diminished in the TME [106, 107]. Moreover, tumor cells are restricted by a dynamic process known as immunoediting, which favors the development of fewer immunogenic tumor cells and the mechanism of tumor escape variants which can evade the immune response and acquire a survival advantage [94]. Tumor immunogenicity is directly associated with anti-tumor T-cell responses, survival benefits and immunotherapy response in HNSCC [18, 108]. Human leukocyte antigen class I molecules play a vital role in cell-mediated immunity, particularly as antigen-presenting molecules of $CD8^+$ cytotoxic T lymphocytes (CTLs), which identify tumor antigen-binding peptides presented by HLA class I molecules on the cell surface and destroy target cancer cells [109, 110]. Some primary HNSCCs have a reduced expression of HLA class I antigens and a further downregulation or complete loss in metastases, frequently related to lower expression of antigen processing machinery (APM) and interferon (IFN) γ signaling components [111]. There is evidence that tumor heterogeneity influences the interaction between tumor, immune and stroma cells, which corresponds with the response of HNSCC patients to anti-PD-1/PD-L1 therapy [112-114].

1.9 Characteristics of MHC-I molecules and antigen processing in cancer

Genes of the major histocompatibility complex (MHC) are located on the short arm of chromosome 6 in humans. The human MHC class I (MHC-I) genes are composed of a heavy chain (HC), encoded by the human leukocyte antigen (HLA)-A, HLA-B and HLA-C, and an invariant light chain known as β2-microglobulin (β2m). The heterodimer requires stabilization by a peptide, which is loaded into the MHC-I peptide-binding groove with the APM components [115]. MHC-I functions as an antigen-presenting molecule in the adaptive immune response. Upon ubiquitination, endogenous antigens were hydrolyzed by the proteasome into 6-30 amino acid fragments, then translocated to the endoplasmic reticulum via the transporter associated with antigen processing (TAP), loaded onto the MHC-I dimer and then explored via the trans-Golgi to the cell surface and presented to $CD8^+$ CTL, thereby inducing immune responses [116-118]. Numerous studies have revealed a loss or downregulation of cell surface MHC-I in cancers of various origins, including NSCLC, breast cancer, prostate cancer, colorectal cancer, HNSCC, hepatocellular carcinoma and melanoma, which was associated with disease progression, reduced numbers of TILs and worse patients outcome [104, 119]. MHC-I-mediated antigen presentation is essential for $CD8^+$ CTL and is a major factor in the formation of the endogenous adaptive immune response and the success of T cell-based cancer immunotherapy. A deregulation of MHC-I makes it possible to restore MHC-I expression and adaptive antitumor immunity [115]. The PI3K/AKT signaling and the MEK/ERK signaling are the two major mediators of several receptor tyrosine kinases targeted by TKI, It has been established that the MEK/ERK pathway negatively infers with the HLA-I protein expression and antigen presentation in many cancer types [120] via ERK export-dependent processes, thereby identifying the pathways responsible for MHC-I upregulation upon kinase inhibition [121-123]. Anti-EGFR antibodies or EGFR/MEK inhibitors reduce MAPK signaling and enhance HLA-I expression in a multitude of tumor types [121, 122, 124]. The pharmacological inhibition of MAPK signaling improved the recognition and killing of T cells and TCR-mimicking antibody peptide/MHC targets and might also increase the efficacy of immunotherapies [122]. It is noteworthy that MHC-I expression varies not just between primary and metastatic sites, but also between cancer cells and/or spatial distribution [125-128].

1.10 Role of the programmed death ligand 1 target for cancer therapy

By recognizing and eliminating pathogens and abnormal cells, including cancer cells, T cell immunity is crucial for maintaining homeostasis in the body. Nevertheless, over-activated,

uncontrolled T cells may also attack normal cells [129]. Suppressive immune checkpoint proteins, including cytotoxic T lymphocyte-associated protein 4 (CTLA-4), programmed death-1 (PD-1; encoded by the PDCD1 gene) and programmed death ligand 1 (PD-L1; encoded by the CD274 gene) maintain the complex regulation of T cell activity under normal physiological conditions [130]. The transmembrane protein PD-L1 can be expressed on the surface of antigen-presenting cells and tumor cells. PD-L1 binds specifically to its receptor PD-1 expressed on lymphocytes such as T cells, B cells and bone marrow cells [131, 132]. PD-L1 can bind to PD-1 expressed on the surface of solid and hematologic tumors [133-135]. High PD-L1 expression in cancer cells, including renal cell carcinoma (RCC) and breast cancer, colorectal cancer, gastric cancer, NSCLC, papillary thyroid cancer, and testicular cancer [136] was associated with a poor prognosis [137]. PD-L1 expression is primarily controlled by MAPK (RAS/RAF/MEK/ERK) and PI3K/Akt pathways as well as by numerous intracellular and extracellular signals [138]. Activation of MAPK pathways, particularly kinases, such as RAS, RAF, MEK and ERK, is crucial for the constitutive upregulation of PD-L1 [139, 140]. The RAS/MEK pathway post-transcriptionally upregulates PD-L1 expression via an increase in mRNA stability mediated by tristetraprolin (TTP) [141]. PD-L1 expression was found to be influenced by oncogenic activation of ERK 1/2. The phosphorylation of these downstream oncogenes of MEK can upregulate the transcription of PD-L1 [140, 142]. The PI3K/AKT/mTOR pathway is an important additional regulator of constitutive PD-L1 expression. However, PD-L1 expression is also increased by activation of the PI3K/AKT signaling pathway via other mechanisms, such as loss of PTEN [143]. Downregulating PI3K, AKT, or mTOR moderately affects PD-L1 expression in glioma, NSCLC, breast, and prostate malignancies [144-146]. Inhibition of these pathways can regulate PD-L1 expression thereby facilitating and enhancing the efficacy of cancer treatment.

2 Aims and objectives

Patients with HNSCC require novel, more efficient therapies based on the limited efficacy of current targeted therapies and immunotherapies. Therefore, this study examines the effect of the treatment with tyrosine kinase inhibitors on ERBB family members and associated pathways as well as immune relevant molecules in different HNSCC cell lines. Next to the *in vitro* and *in situ* experiments, *in silico* analyses of TCGA data were performed with particular focus on immune relevant molecules of HNSCC in the context of the immune cell infiltration. HNSCC specimens were analyzed to assess changes in the composition of immune cell subpopulation in primary and metastatic tumors, as well as in the tumor center and tumor margin. Therefore, following questions were addressed:

1) Is there a correlation between the EGFR, HLA-I and APM component expression in HNSCC?

2) Does TKI treatment change the expression of EGFR as well as its downstream AKT and ERK in different HNSCC cell lines?

3) Does TKI treatment alter the expression of the immune-related genes HLA-ABC and PD-L1 in HNSCC cell lines?

4) Is there a difference in the frequency and spatial distribution of immune cell subpopulations in HNSCC tissue sections?

3 Materials and Methods

3.1 Materials

3.1.1 Chemicals and plastic ware

3.1.1.1 Chemicals

Materials	Distributor
0.5% Trypsin-EDTA (10x)	Gibco® Invitrogen, Carlsbad, USA
1 x plus Amplification Diluent	PerkinElmer, Waltham, USA
2 X SYBR qPCR Master Mix	Nanjing Vazyme Biotech, Nanjing, China
Agarose	SERVA Electrophoresis GmbH, Heidelberg, Germany
Amphotericin B	c.c.pro GmbH, Oberdorla, Germany
Ampuwa® water	Fresenius Kabi GmbH, Bad Homburg, Germany
Antigen Retrieval Reagent, pH6（10X）	PerkinElmer, Waltham, USA
Antigen Retrieval Reagent, pH9（10X）	AKOYA Biosciences, Marlborough, USA
BCA Protein Assay Reagent	Thermo Fisher Scientific, Waltham, USA
Bolt™ 4-12% Bis-Tris Plus Gel	Thermo Fisher Scientific, Waltham, USA
Bovine Serum Albumin (BSA)	Sigma-Aldrich GmbH, St. Louis, USA
CCL5 Elisa Kit	Biolegend, San Diego, USA
Cell Proliferation Kit II (XTT)	Sigma-Aldrich GmbH, St. Louis, USA
CXCL10 (IP10) Elisa Kit	Biolegend, San Diego, USA
Dimethyl sulfoxide (DMSO)	CARL ROTH GmbH & Co. KG, Karlsruhe, Germany
Dulbecco's Phosphate Buffered Saline (PBS)	Sigma-Aldrich GmbH, St. Louis, USA
Dulbecco's Modified Eagle Medium (DMEM)	Gibco® Invitrogen, Carlsbad, USA
Erlotinib	LC Laboratories, Woburn, USA
Ethanol absolute for analysis	Sigma-Aldrich GmbH, St. Louis, USA
Ethylene diamine tetra-acetic acid (EDTA)	Sigma-Aldrich GmbH, St. Louis, USA
Fetal bovine Serum (FBS)	Anprotec, Bruckberg, Germany
GeneRuler DNA Ladder	Thermo Fisher Scientific, Waltham, USA
Halt™ Protease & Phosphatase inhibitor Cocktail (100X)	Thermo Fisher Scientific, Waltham, USA
iBlot 2 Dry Blotting System	Thermo Fisher Scientific, Waltham, USA
iBlot™ 2 NC Regular Stacks	Thermo Fisher Scientific, Waltham, USA
Lapatinib	LC Laboratories, Woburn, USA

L-glutamine	Lonza, Basel, Switzerland
MES SDS Running Buffer (20X)	Thermo Fisher Scientific, Waltham, USA
Methanol	CARL ROTH GmbH & Co. KG, Karlsruhe, Germany
Minimum Essential Medium (MEM)	Gibco® Invitrogen, Carlsbad, USA
Minimum Essential Medium Non-Essential Amino Acids (MEM NEAA,100x)	Gibco® Invitrogen, Carlsbad, USA
Natriumchlorid (NaCl) sodium chloride	CARL ROTH GmbH & Co. KG, Karlsruhe, Germany
Nonylphenol-40 (NP-40)	Sigma-Aldrich GmbH, St. Louis, USA
NucleoSpin RNA isolation kit	Machery-Nagel, Düren, Germany
Opal Antibody Diluent/Block	AKOYA Biosciences, Marlborough, USA
Opal Fluorophore Reagent Packs	AKOYA Biosciences, Marlborough, USA
p44/42 MAPK (Erk1/2) Antibody	Cell Signaling, Danvers, USA
PageRuler™ Prestained Protein Ladder	Thermo Fisher Scientific, Waltham, USA
Parafilm	IDL GmbH & Co. KG, Nidderau, Germany
Penicillin-Streptomycin Mix	Sigma-Aldrich GmbH, St. Louis, USA
Polysorbate 20 (Tween 20)	AppliChem GmbH, Darmstadt, Germany
Ponceau S	AppliChem GmbH, Darmstadt, Germany
Potassium Chloride - KCl	AppliChem GmbH, Darmstadt, Germany
Potassium phosphate monobasic - KH_2PO_4	Merck, Darmstadt, Germany
RevertAid First Strand cDNA synthesis kit	Thermo Fisher Scientific, Waltham, USA
RNA isolation kit	Macherey & Nagel, Düren, Germany
ROTI® Histofix 4,5 % Formaldehyd, PH 7	CARL ROTH GmbH & Co. KG, Karlsruhe, Germany
RPMI 1640 media	Gibco® Invitrogen, Carlsbad, USA
SignalFire ECL Reagent	Cell Signaling, Danvers, USA
Skim milk powder	BD Biosciences, Heidelberg, Germany
Sodium phosphate dibasic dihydrate ($Na_2HPO_4 * 2H_2O$)	CARL ROTH GmbH & Co. KG, Karlsruhe, Germany
Spectral DAPI	AKOYA Biosciences, Marlborough, USA
Tris Ultrapure	AppliChem GmbH, Darmstadt, Germany

VECTASHIELD® HardSet™ Antifade Mounting Medium for fluorescence	VECTOR Laboratories, Newark, USA
Xylol /ROTICLEAR	CARL ROTH GmbH & Co. KG, Karlsruhe, Germany
β-Mercaptoethanol	AppliChem GmbH, Darmstadt, Germany

3.1.1.2 Consumables and plastic ware

Name	**Company**
0.2 mL Thin Wall PCR Tubes	Greiner Bio-One GmbH, Frickenhausen, Germany
12 well plate (flat bottom)	SARSTEDT AG & Co. KG, Nümbrecht, Germany
15 mL tubes	SARSTEDT AG & Co. KG, Nümbrecht, Germany
24 well plate (flat bottom)	SARSTEDT AG & Co. KG, Nümbrecht, Germany
25, 75 and 175 cm^2 cell culture flasks	SARSTEDT AG & Co. KG, Nümbrecht, Germany
50 mL tubes	SARSTEDT AG & Co. KG, Nümbrecht, Germany
6 well plate (flat bottom)	SARSTEDT AG & Co. KG, Nümbrecht, Germany
96 well plate (flat bottom)	SARSTEDT AG & Co. KG, Nümbrecht, Germany
Counting chambers	Paul Marienfeld GmbH & Co. KG, Marienfeld, Germany
Coverslips (24 x 32 mm)	CARL ROTH GmbH & Co. KG, Karlsruhe, Germany
FACS tubes	SARSTEDT AG & Co. KG, Nümbrecht, Germany
Multiplate PCR Plates,96-well	Bio-Rad, Hercules, USA
Pipette tips (0-10 µL, 10-100 µL, 20-200 µL, 100-1000 µL)	SARSTEDT AG & Co. KG, Nümbrecht, Germany
Pipettes	Eppendorf AG, Hamburg, Germany
Safe seal micro tube 1.5 mL, PP	SARSTEDT AG & Co. KG, Nümbrecht, Germany
Safe seal micro tube 2.0 mL, PP	SARSTEDT AG & Co. KG, Nümbrecht, Germany
Super PAP Pen（liquid blocker）	Kisker Biotech GmbH & Co.KG, Steinfurt, Germany
5 mL, 10 mL, 25 mL, 50 mL sterile pipets	Greiner Bio-One GmbH, Kremsmünster, Austria

3.1.1.3 Antibodies

A. Antibodies used for flow cytometry

Name	Fluorophore	Company
Anti-CD274 (PD-L1)	PE	Invitrogen eBioscience ™, Carlsbad, USA
Anti-EGFR	PE	BD Biosciences, Heidelberg, Germany
Anti-ERBB2	PE	BD Biosciences, Heidelberg, Germany
Anti-HLA-ABC	PE	Invitrogen eBioscience ™, Carlsbad, USA

B. Antibodies used for Western Blot analysis

Antibody	Dilution	Source	Company
Primary antibodies			
AKT	1:1000	Rabbit	Cell Signaling, Danvers, USA
EGFR	1:1000	Rabbit	Cell Signaling, Danvers, USA
GAPDH	1:1000	Rabbit	Cell Signaling, Danvers, USA
HC10	1:500	Mouse	From Soldano Ferrone, Boston, USA
p44/42 MAPK (ERK1/2)	1:1000	Rabbit	Cell Signaling, Danvers, USA
Phospho-AKT	1:1000	Rabbit	Cell Signaling, Danvers, USA
Phospho-EGFR	1:1000	Rabbit	Cell Signaling, Danvers, USA
Phospho-p44/42 MAPK (ERK1/2)	1:1000	Rabbit	Cell Signaling, Danvers, USA
Secondary antibodies			
Anti-mouse IgG, HRP-linked antibody	1:1000	Horse	Cell Signaling, Danvers, USA
Anti-rabbit IgG, HRP-linked antibody	1:1000	Goat	Cell Signaling, Danvers, USA

C. Antibodies used for multiplex immunohistochemistry

Name	Dilution	Company
Primary antibodies		
CD163 (MRQ-26)	1:50	Cell Marque, Rocklin, USA
CD20 (L26)	1:400	DAKO, Glostrup, Danmark
CD3 (SP7)	1:100	Thermo Fisher Scientific, Waltham, USA
CD8 (SP16)	1:100	Abcam, Cambridge, UK
Foxp3 (236A/E7)	1:100	Abcam, Cambridge, UK
panCK (AE1/AE3)	1:100	DAKO, Glostrup, Danmark
Secondary antibody		
Opal Polymer HRP mouse + rabbit, PerkinElmer, Waltham, USA		

3.1.1.4 Buffers

Buffer	Component
5% BSA buffer	Dissolve 5g of BSA in 100 mL of TBST, with 0.01% NP-40.
PBST	1000mL PBS with 0.5mL Tween-20 solution
Phosphate-buffered saline (PBS), pH 7.4	70 mM NaCl (AppliChem GmbH), 1.5 mM KCl (AppliChem GmbH), 750 nM KH_2PO_4 (Sigma-Adrich GmbH), 400 nM Na_2HPO_4 (Sigma-Adrich GmbH).
Radioimmunoprecipitation assay (RIPA) buffer	25 mM Tris HCl (pH 7,6), 150mM NaCl, 1% (v/v) NP-40, 1% (w/v) sodium deoxycholate, 0.1% (w/v) SDS
TAE (50-fold)	2 M Tris, 0.05 M EDTA, 5.7 % (v/v) acetic acid
TBS (10-fold)	0.2 M Tris, 1.4 M NaCl (pH 7.6 with HCl)
TBST	100 mL 10-fold TBS, 900 mL H_2O, 1 mL Tween-20-solution

3.1.2 Equipments and Softwares

3.1.2.1 Equipment

Name	Company
96-well labcycler gradient	SensoQuest GmbH, Göttingen, Germany
Allegra X-15R Centrafuge	Beckman Coulter, Krefeld, USA
Biometra® Power Pack P25 T	Biometra GmbH, Göttingen, Germany
Centrifuge 5414C	Eppendorf AG, Hamburg, Germany
CFX Connect™ Real-time system	Bio-Rad, Hercules, USA
CO_2 Incubator	BINDER GmbH, Tuttlingen, Germany
Cold centrifuge 5425R	Eppendorf AG, Hamburg, Germany
Evos FLoid™ Imaging System	Thermo Fisher Scientific, Waltham, USA
Heraeus Incubator	Heraeus Company, Bitterfeld-Wolfen, Germany
iBlot™ 2 Gel Transfer Device	Thermo Fisher Scientific, Waltham, USA
Infinite® 200Pro microplate reader	Tecan Group Ltd., Mannedorf, Switzerland
LAS 3000 CCD camera system	FujiFilm, Tokyo, Japan
Manitowoc ice maker	Manitowoc Company, Manitowoc, USA
Mini Gel Tank	Thermo Fisher Scientific, Waltham, USA
MMM Medcenter™ Venticell™ Drying Ovens	MMM Medcenter Company, Planegg, Germany
Navios flow cytometer	Beckman Coulter, Krefeld, Germany
PowerPac™ Basic Power Supply	Bio-Rad, Hercules, USA
Rotor-Gene	Qiagen, Venlo, Netherlands
SimpliAmp™ Thermal Cycler	Thermo Fisher Scientific, Waltham, USA
Thermomixer F1.5	Eppendorf AG, Hamburg, Germany
Vectra Polaris	PerkinElmer, Waltham, USA

Vectra Polaris Automated Quantitative Pathology Imaging System	PerkinElmer, Waltham, USA
VILBER Gel Documentation system	VILBER Company, Eberhardzell, Germany

3.1.2.2 Software

Software	**Company**
Acrobat Reader DC	Adobe, San Jose, USA
Adobe Photoshop CC 2015.5	Adobe, San Jose, USA
Bio-Rad CFX	Bio-Rad, Hercules, USA
Endnote X9	Thomson Reuters, Canada
FlowJo_V10.8.1	DONGLE
GraphPad Prism 9.0.0	GraphPad Software, San Diego, USA
Image Reader LAS3000 software	Fuji GmbH, Düsseldorf, Germany
ImageJ 1.53k	National Institute of Health, Bethesda, USA
inForm Tissue Finder	AKOYA Biosciences, Marlborough, USA
Kaluza® Flow Analysis Software	Beckman Coulter, Krefeld, USA
Microsoft Excel 2019	Microsoft, Redmond, USA
Microsoft PowerPoint 2019	Microsoft, Redmond, USA
Microsoft Word 2019	Microsoft, Redmond, USA
OriginPro 2021	OriginLab, Northampton, USA
Rstudio Desktop	Rstudio company, Boston, USA
R2 Genomics Analysis and Visualization Platform	https://hgserver1.amc.nl/cgi-bin/r2/main.cgi?open_page=login
Xenabrowser	UCSC Xena (xenabrowser.net)
ScienceSlide 2016	VisiScience, Inc.

3.2 Methods

3.2.1 Cell culture

3.2.1.1 Cell lines and cell culture

The HNSCC cell lines PCI-1, PCI-4A, PCI-4B, PCI-13, PCI-15B, PCI-30, PCI-31, PCI-52, SCC4, CAL33, XF354, SAS and FaDu were obtained from Prof. Theresa L. Whiteside (University of Pittsburgh, USA) and maintained in Roswell Park Memorial Institute 1640 medium (RPMI 1640, Gibco® Invitrogen, Carlsbad, USA) or Dulbecco's Modified Eagle Medium (DMEM, Gibco® Invitrogen) supplemented with 10% (v/v) inactivated fetal bovine serum (Anprotec, Bruckberg, Germany), 1% (v/v) penicillin (Sigma-Aldrich GmbH, St. Louis, USA) and 1% (v/v) L-glutamine (200mM, Lonza, Basel, Switzerland) in a 5% CO_2 atmosphere at 37℃. A pair of HNSCC cell lines from the same patient, the primary tumor cell line UH-SCC-17A and the metastatic UH-SCC-17B obtained from a lymph node metastasis were provided by Prof. Tuula Salo at the Department of Oral and Maxillofacial Diseases-University of Helsinki (Helsinki, Finland)) and cultured in

Minimum Essential Medium (MEM) supplemented with 10% fetal bovine serum, 1% (v/v) penicillin, 1% (v/v) L-glutamine, 1% (v/v) MEM NEAA (Gibco® Invitrogen) and 0.1% (v/v) Amphotericin B (c.c.pro, Oberdorla, Germany).

Table 1. Characteristic of the HNSCC cell lines

Cell line	Sex	Age	Specimen site	Type	Culture medium
UH-SCC-17A	Male	50	Mobile tongue	Primary	Minimum Essential Medium (MEM)
UH-SCC-17B	Male	50	Neck	Metastasis	
PCI-1	Male	65	Larynx	Primary	Dulbecco's Modified Eagle Medium (DMEM)
PCI-4A	Male	51	Larynx	Primary	
PCI-4B	Male	51	Larynx	Metastasis	
PCI-13	Male	50	Oral cavity	Primary	
PCI-15B	Male	69	Hypopharynx	Metastasis	
PCI-30	Male	54	Oral tongue	Primary	
PCI-31	Male	48	Oral cavity	Primary	
PCI-52	Male	43	Larynx	Primary	
SCC4	Male	55	Oral tongue	Primary	
CAL33	Male	69	Oral tongue	Primary	Roswell Park Memorial Institute 1640 medium (RPMI 1640)
SAS	Female	69	Oral tongue	Primary	
XF354	Male	51	Oral cavity	Primary	
FaDu	Male	56	Hypopharynx	Primary	

When the cells were approximately 80% confluent, the used culture medium was removed, cells were washed once with PBS followed by adding 0.5% Trypsin-EDTA (10X) diluted 1:7 with PBS. The digestion was stopped when the cells were no longer attached to the flask wall using fresh medium. The cell concentration was measurement by counting the cells using a counting chamber (Paul Marienfeld GmbH & Co. KG, Marienfeld, Germany). The average number of viable cells in each of the four sets of 16 squares were multiplied by 10,000 to determine the number of cells per milliliter. This number was multiplied according to the 1:5 dilution from the trypan blue addition. For long-term storage, cells were counted to ensure the cell viability (> 90%) and then spun down at 300rpm for 5 minutes and the medium was removed. The cells were resuspended in the freezing medium (freezing medium: 90% FBS (fetal bovine serum) with 10% (v/v) DMSO) followed by -80°C overnight storage prior to permanent storage in liquid nitrogen.

3.2.1.2 Mycoplasma detection

After three days of cell culture, 200 µL of cell culture supernatant was heated at 95°C for 5 minutes and centrifuged at 12000 x g for 10 minutes. The supernatant was used as template to extract DNA and initiate PCR reaction with mycoplasma-specific primers (Table 2).

Table 2. Primers used for mycoplasma detection

Name	Sequence	Concentration of primer mix
5′ primer	5′-CGCCTGAGTAGTACGTTCGC-3′ 5′-CGCCTGAGTAGTACGTACGC-3′ 5′-TGCCTGGGTAGTACATTCGC-3′ 5′-TGCCTGAGTAGTACATTCGC-3′ 5′-CGCCTGAGTAGTATGCTCGC-3′ 5′-CACCTGAGTAGTATGCTCGC-3′ 5′-CGCCTGGGTAGTACATTCGC-3′	5 µmol/L per primer
3′ primer	5′-GCGGTGTGTACAAGACCCGA-3′ 5′-GCGGTGTGTACAAAACCCGA-3′ 5′-GCGGTGTGTACAAACCCCGA-3′	5 µmol/L per primer

The PCR reaction mixture and procedure are as follows:

Reaction mixture:

2x SYBR master mix	12.5 µL
Forward primer	0.5 µL
Reverse primer	0.5 µL
ddH2O	6.5 µL
sample	5 µL

Reaction procedure:

Temperature	Time	Number of Cycle
95℃	10 minutes	40
95℃	45 seconds	
58℃	1 minutes 30 seconds	
72℃	1 minutes 30 seconds	
72℃	5min	1
25℃	∞	

1.3% (w/v) agarose gel was prepared using TAE (40 mM Tris-acetate, 1 mM EDTA) solution with ethidium bromide (EtBr, 0.5 µg/mL). Fill the gel run chamber with 1x TAE buffer until the gel is completely covered. 5 µL of DNA sample mixed with an equal volume of loading buffer

was added to each well, the test samples, a positive control, and a DNA marker were loaded onto the gel and run at 95 V for one hour and the results were captured using ultraviolet transilluminator.

3.2.2 Total RNA isolation, reverse transcription and real-time PCR

3.2.2.1 RNA isolation

Total RNA was isolated from HNSCC cell lines using RNA Isolation kit (Macherey & Nagel, Düren, Germany) according to manufacturer's instructions. Briefly, cell samples were removed from the -80°C freezer and placed on ice. The cell pellet was immediately treated with the lysis buffer from RNA isolation Kit supplemented with 1% (v/v) β-mercaptoethanol (AppliChem GmbH, Darmstadt, Germany). RNA was extracted from the cell lysate using the NucleoSpin RNA Isolation Kit according to the manufacturer's instructions. The RNA concentration was determined using the Infinite 200 PRO Microplate Reader (Tecan Group Ltd., Mannedorf, Switzerland) and NanoQuant Plate™ (Atlantic Lab Equipment, Beverly, USA) with Ampuwa water (Fresenius Kabi, GmbH, Bad Homburg, Germany) as blank, and spectrometric measurements of absorbance at 260 nm. Initially, the purity of the total RNA was assessed by comparing the absorbances at 260 and 280 nm. Only samples with a ratio value of close to 2 were utilized. The isolated RNA was stored at -80 °C or immediately used for cDNA synthesis.

3.2.2.2 cDNA synthesis

For cDNA production, 0.5 µg RNA was diluted to a final volume of 11 µL by adding RNase-free water and then 1µL of 100 mM Oligo(dT) primer was added and incubated at 65°C for 5 minutes to denature the secondary structure of the RNA template. After a quick chill on ice, reverse transcription (RevertAid First Strand cDNA synthesis kit, Thermo Fisher Scientific) was performed as follows:

RNA template	12 µL
5X Reaction Buffer	4 µL
dNTP Mix (10 mM)	2 µL
RiboLock Rnase Inhibitor (20 U/µL)	1 µL
RevertAid RT (200 U/µL)	1 µL
Total volume	20 µL

3.2.2.3 Quantitative PCR

Gene expression was quantified by quantitative PCR (qPCR) using 2x SYBR Green qPCR Master Mix (Nanjing Vazyme Biotech, China) and cDNA. PCRs were performed in a standard 96-well plate format with a CFX Connect Real-Time System and Bio-Rad CFX Maestro software (both from Bio-Rad, Hercules, CA, USA).

The PCR reaction solution was prepared as follows:

2x ChamQ Universal SYBR qPCR Master Mix	10 μL
Forward primer(10μM)	0.5 μL
Reverse primer (10μM)	0.5 μL
cDNA	1 μL
ddH_2O	8 μL

The PCR amplification method is as described below:

	Temperature	**Time**	**Number of Cycle**
Pre-denaturation	95 ℃	3 minutes	1
Denaturation	95 ℃	10 seconds	45
Annealing + extension	60 ℃	30 seconds	
Melt curve	95 ℃	15 seconds	1
	60 ℃	60 seconds	
	95 ℃	15 seconds	

Primers (Table 3) were acquired from publications or from the PrimerBank. RNA relative abundance changes were evaluated using the $2^{-\Delta\Delta Cq}$ method. The housekeeping gene delta-aminolevulinate synthase 1 (ALAS1) was used for normalization.

Table 3. Primers for qPCR analysis

Gene	**Sequence**	**Tm**
EGFR	Forward Primer: 5'-TTGCCGCAAAGTGTGTAACG-3'	62
	Reverse Primer: 5'-GTCACCCCTAAATGCCACCG-3'	63
ERBB2	Forward Primer: 5'-TGGCCTGTGCCCACTATAAG-3'	61
	Reverse Primer: 5'-AGGAGAGGTCAGGTTTCACAC-3'	61
HLA-ABC	Forward Primer: 5'-GCCTACCACGGCAAGGATTAC-3'	60
	Reverse Primer: 5'-GGTGGCCTCATGGTCAGAGA-3'	60
PD-L1	Forward Primer: 5'-GCTGCACTAATTGTCTATTGGGA-3'	62
	Reverse Primer: 5'-AATTCGCTTGTAGTCGGCACC-3'	60
CCL5	Forward Primer: 5'-CCTGCTGCTTTGCCTACATTGC-3'	63
	Reverse Primer: 5'-ACACACTTGGCGGTTCTTTCGG-3'	62
CXCL10	Forward Primer: 5'-CCACGTGTTGAGATCATTGCT-3'	61
	Reverse Primer: 5'-TGCATCGATTTTGCTCCCCT-3'	61

CCL2	Forward Primer: 5'-CAGCCAGATGCAATCAATGCC-3'	62
	Reverse Primer: 5'-TGGAATCCTGAACCCACTTCT-3'	60
CCL22	Forward Primer: 5'- ATCGCCTACAGACTGCACTC-3'	61
	Reverse Primer: 5'- GACGGTAACGGACGTAATCAC-3'	61
CXCL9	Forward Primer: 5'-CCAGTAGTGAGAAAGGGTCGC-3'	62
	Reverse Primer: 5'- AGGGCTTGGGGCAAATTGTT-3'	63
TGFβ1	Forward Primer: 5'-GGCCAGATCCTGTCCAAGC-3'	62
	Reverse Primer: 5'-GTGGGTTTCCACCATTAGCAC-3'	62
TGFβ2	Forward Primer: 5'-CAGCACACTCGATATGGACCA-3'	62
	Reverse Primer: 5'-CCTCGGGCTCAGGATAGTCT-3'	62
TGFβ3	Forward Primer: 5'-ACTTGCACCACCTTGGACTTC-3'	63
	Reverse Primer: 5'-GGTCATCACCGTTGGCTCA-3'	62
TGFβR1	Forward Primer: 5'-ACGGCGTTACAGTGTTTCTG-3'	61
	Reverse Primer: 5'-GCACATACAAACGGCCTATCTC-3'	61
TGFβR2	Forward Primer: 5'-GTAGCTCTGATGAGTGCAATGAC-3'	61
	Reverse Primer: 5'-CAGATATGGCAACTCCCAGTG-3'	60
TGFβR3	Forward Primer: 5'-TGGGGTCTCCAGACTGTTTTT-3'	61
	Reverse Primer: 5'-CTGCTCCATACTCTTTTCGGG-3'	60
ALAS1	Forward Primer: 5'-CGCCGCTGCCCATTCTTAT-3'	63
	Reverse Primer: 5'-TCTGTTGGACCTTGGCCTTAG-3'	61

3.2.3 Western blot analysis

3.2.3.1 Protein extraction and measurement of protein concentration

5×10^5-1 x 10^7 cells were washed twice with 5 mL of ice-cold PBS and centrifuged (300xg, 5 min, 4°C) for protein extractions. The resultant cell pellets were resuspended, transferred to 1.5 mL Eppendorf Safe-Lock reaction tubes and centrifuged again (300 x g, 5 min, 4°C). After discarding the supernatant, cell pellets were immediately frozen at -80°C. For cell lysis and DNA destruction, cells were resuspended in RIPA buffer containing a fresh protease and phosphatase inhibitor cocktail (1:100, Thermo Fisher Scientific, *Waltham,* USA) and sonicated twice (Bandelin HD 2070 Sonoplus equipped with an MS 73 micro needle) with at least five pulses (1 second pause) and 70% intensity. The cell lysate was placed on ice for 5 minutes then centrifuged (12,000 x g, 30 minutes, 4°C) to remove fragments before the supernatant was transferred into a new 1.5 mL sterile reaction tube. The protein concentration was quantified using an Infinite® 200Pro absorbance microplate reader (TECAN) and the Pierce BCA kit (Thermo Fisher Scientific) according to the manufacturer's instructions. Using eight predetermined bovine serum albumin (BSA) standards (range from 0 to 2 mg/mL) were utilized to generate the associated calibration curves. The lysates were further supplemented with 4x Laemmli buffer containing 10% (v/v) -mercaptoethanol (AppliChem GmbH, Darmstadt,

Germany) and heated for 5 min at 95°C before loading onto Bolt™ 4-12% Bis-Tris Plus Gels (Thermo Fisher Scientific) for Western blot analysis.

3.2.3.2 Gel electrophoresis, blotting, staining

For Western Blot analysis, 15 - 30 µg of protein (Using BCA Protein Assay Kit (Thermo Scientific) to measure the protein concentration) were separated on Bolt™ 4-12% Bis-Tris Plus Gels using Wet Tank Transfer System (Thermo Fisher Scientific) for Western blot analysis. A prestained protein ladder (Thermo Fisher Scientific) was used as molecular weight marker. The samples were run at a voltage of 100V until the dye reached the bottom edge and then transferred using the iBlot™ 2 Dry Blotting System (Thermo Fisher Scientific) and iBlot™ 2 Transfer Stack (Thermo Fisher Scientific) under P0 program (20V 1 min, 23V 4 min, 25V 2min) (Trans-Blot® Tank, BIO-RAD, Laboratories, Inc, California, USA) onto nitrocellulose. The membranes were then stained with Ponceau S (AppliChem GmbH, Darmstadt, Germany) staining solution (0.2% (w/v) Ponceau S in 3% (w/v) TCA), and thoroughly rinsed with water and TBST. The membranes were blocked for 1 hours with 5% skim milk (w/v) diluted in TBS-T (0.2 M Tris, 1.4 M NaCl, 0.2% Tween, pH 7.6) and then incubated with target-specific primary rabbit or mouse antibodies (Abs) (§ 3.1.1.3) to bind proteins on the membrane. As loading controls, we used anti-GAPDH specific antibody (Ab) (Cell Signaling, Danvers, USA). After primary Ab incubation, membranes were washed three times at room temperature with TBS-T and stained with anti-rabbit or anti-mouse horseradish peroxidase (HRP)-conjugated secondary Ab (Cell Signaling). Membranes were incubated with primary or secondary Ab as specified by the manufacturer. Positive signals were detected using enhanced chemiluminescence substrate SignalFire™ ECL Reagent (Cell Signaling) and captured with Fuji LAS3000 camera (Fuji GmbH, Düsseldorf, Germany). The digitized immunostaining signals were then analyzed and quantified using the ImageJ software (National Institute of Health, Bethesda, USA).

3.2.4 Cell proliferation assay

Cells were seeded at a density of $6x10^3$ cells per well in 100 µL of phenol red-free culture medium in 96-well plates one day prior, and then incubated with various concentrations of lapatinib and erlotinib in 200 µL medium for 48 hours. The cytotoxic activity of the drug was evaluated using the XTT (Cell Proliferation Kit II, Sigma-Aldrich) assay. Prior to the experiments, XTT measurement solution was prepared using 1 mL of sodium 3’-[1-(phenylaminocarbonyl)-3,4-tetrazolium]-bis (4-methoxy-6-nitro) benzene sulfonic acid hydrate (XTT labeling reagent) in combination with 20 µL of N-methyl dibenzopyrazine methyl sulfate (PMS, Electron

coupling reagent). After incubation, a mixture of 50 µL XTT labeling solution was added to each well, and the plates were incubated for four hours in the cell incubator. The absorbance was measured at 490 nm and 630 nm using a TECAN microplate reader. The evaluation is based on the means of at least three independent experiments, with at least three replicates per incubation concentration. The cytotoxic effects of drugs and their combinations were determined and dose-response curves were drawn using GraphPad Prism 9 (GraphPad Software, San Diego, CA, USA).

3.2.5 Multiplex immunohistochemistry

For immunohistochemical staining, each slide was incubated at 60 ℃ for 60 minutes, dewaxed with xylene (3x 10min), and rehydrated in a series of decreasing concentration ethanol solutions (100% 1x 5min; 95% 1x 5min; 70% 1x 5min; 50% 1x 5min; 25% 1x 5min). After rehydrating, the slides were rinsed in distilled water, fix them in 10% neutral formalin for 20 minutes, and then rinse them briefly in distilled water.

The protocol for multiplex immunostaining is depicted below:

	CD20	CD80	Foxp3	CD3	CD163	panCK	Nuclei DAPI
AR buffer Time	PH6 15min	PH6 15min	PH9 15min	PH6 15min	PH6 15min	PH6 15min	PH6 15min
Wash	dH_2O, TBST						
Block	10min, RT						-
Primary Antibody	CD20 1:400 30min	CD8 1:100 45min	Foxp3 1:100 30min	CD3 1:100 30min	CD163 1:50 30min	panCK 1:100 45min	DAPI
Wash	TBST, 3 times						
Secondary Antibody	Opal Polymer HRP Ms + Rb, 10min RT						-
Wash	TBST, 3 times						dH_2O
Opal Time	520 10min	570 10min	540 10min	650 10min	620 10min	690 10min	-
Wash	TBST, 3 times						-

Place slides in the appropriate antigen retrieval (AR) buffer (pH 6 or pH 9), boil them in water (above 99℃) for 15 minutes and then allow them to cool to room temperature. The slides were washed with distilled water (one time) and TBST (one time), and the tissue section was encircled using a hydrophobic barrier PAP Pen, the tissue sections were covered with blocking buffer (AKOYA Biosciences, Marlborough, USA) and the slides were incubated in a wet

chamber for 10 minutes with shaking at room temperature. Then the blocking buffer was removed, the primary antibody was mixed with the blocking buffer followed by adding the antibody mixture to the slides and incubating according to the protocol's instructions. The primary Ab was removed from the slides by washing with TBST three times for two minutes, then incubate the slides at room temperature for 10 minutes with a secondary antibody (HRP Ms + Rb, PerkinElmer) by ensuring that the reagent covers the tissue region. The slides were incubated with the Opal reagent (AKOYA Biosciences, diluted with 1 x amplification diluent) for 10 minutes, drain off opal reagent and wash with TBST (3 x 2 minutes), water bath slides with AR buffer for 15 minutes, allow them to cool to room temperature, and repeat the procedure for the next antibody. Finally, incubate slides with DAPI (AKOYA Biosciences, 2 drops in 1 mL TBST) for 5 minutes to stain the nuclei. Then the slides were washed with TBST (3 x 2 minutes) and with distilled water for 2 minutes and dry the slides, covered with cover slips.

3.2.6 Analysis of multiple staining

The slides were scanned using Vectra Quantitative Pathology Imaging Systems and further analyzed with inform and Rstudio software (Figure 3).

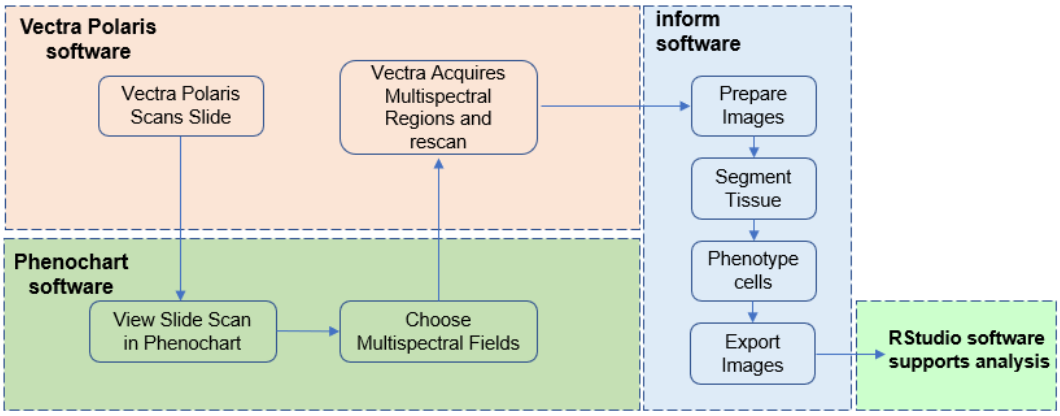

Figure 3. Multispectral Workflow. Vectra Polaris scans the slide to obtain the whole field of view of the slide, and then uses Phenochart software to select the area that needs further analysis and then uses the inform software to mark cells labeled with different Ab and display them in different colors. The output image is further analyzed by RStudio to obtain experimental results.

3.2.7 Flow cytometric analysis

Flow cytometry analysis was conducted using a panel of phycoerythrin (PE)-conjugated antibodies in accordance with the manufacturer's instructions. $2x10^5$ cells were harvested by trypsinization, washed twice with PBS (300xg, 5 min, 4°C), incubated with an appropriate

volume of the corresponding Ab for 20 minutes at room temperature or 30 minutes at 4°C, and subsequently analyzed by flow cytometry. Measurements were performed on a Navios (Beckman Coulter, Krefeld, Germany) flow cytometer. The obtained data were then analyzed using flow analysis software (Beckman Coulter). Histograms depict the mean fluorescence intensity (MFI) of cell surface markers.

3.2.8 Enzyme-linked immunosorbent assay (ELISA)

Cultured supernatant collected from the control and treatment group after 48 h was evaluated by CCL5 and CXCL10 ELISA kits (Biolegend, San Diego, USA) according to manufacturer's instruction. The absorbance at 450nm was measured by Infinite 200Pro microplate reader (Tecan Group Ltd.).

3.2.9 TCGA database analysis

The TCGA expression data for HNSCC were downloaded from UCSC XENA and matched with clinical data. Marker genes for 22 immune cells were retrieved from the Cibersort website, and the R code for Cibersort was used to calculate immune cells. Analysis of immune cell differences between tumor and normal samples based on RNA-seq data from HNSCC samples obtained from UCSC XENA (502 tumor vs. 44 normal samples). Gene correlation analysis was performed with the R2: Genomics Analysis and Visualization Platform (http://r2.amc.nl) and correlation statistics were shown as Pearson correlation coefficients. The clinical correlation of HLA class I antigens, APM components, PD-L1, TGFβ family as well as ERBB protein family members (EGFR, ERBB2, ERBB3 and ERBB4) were analyzed. The number of samples investigated and the datasets utilized are as follows: Tumor Head and Neck Squamous Cell Carcinoma - TCGA - 520 samples.

3.2.10 Statistical analysis

There were at least three independent biological replicates for each experiment. The results are expressed as the mean of at least three independent experiments, along with the corresponding standard deviation or standard error. The statistical significance of differences between experiments was determined using two-tailed t-tests on statistically evaluated data. Unless otherwise specified, paired or unpaired t-tests were used, and Welch's correction was applied to unpaired t-tests when the F-test variance of the two data sets was heterogeneous. Statistical significance was determined by p-values of $p < 0.05$ (*), $p < 0.01$ (**), $p < 0.001$ (***), and $p < 0.0001$ (****).

4 Results

4.1 Connection between the ERBB protein family and the immunological evasion phenotype

It has recently been postulated that overexpression and/or activation of signal transduction molecules are involved in a reduced immunogenicity of different tumor types, including HNSCCs [106, 147]. To determine whether the expression of ERBB family members is associated with the immune escape phenotype, the expression of EGFR, ERBB2, ERBB3 and ERBB4 and different immune modulatory molecules was determined using *in silico* analysis of the human TCGA HNSCC dataset "Tumor Head Neck Squamous Cell Carcinoma" consisting of 520 samples and their expression patterns were correlated to each other. As shown in Figure 4, the correlation of HER family members to HLA class I, HLA class I APM and IFN signal components, the non-classical HLA class I antigens and PD-L1 was highly variable.

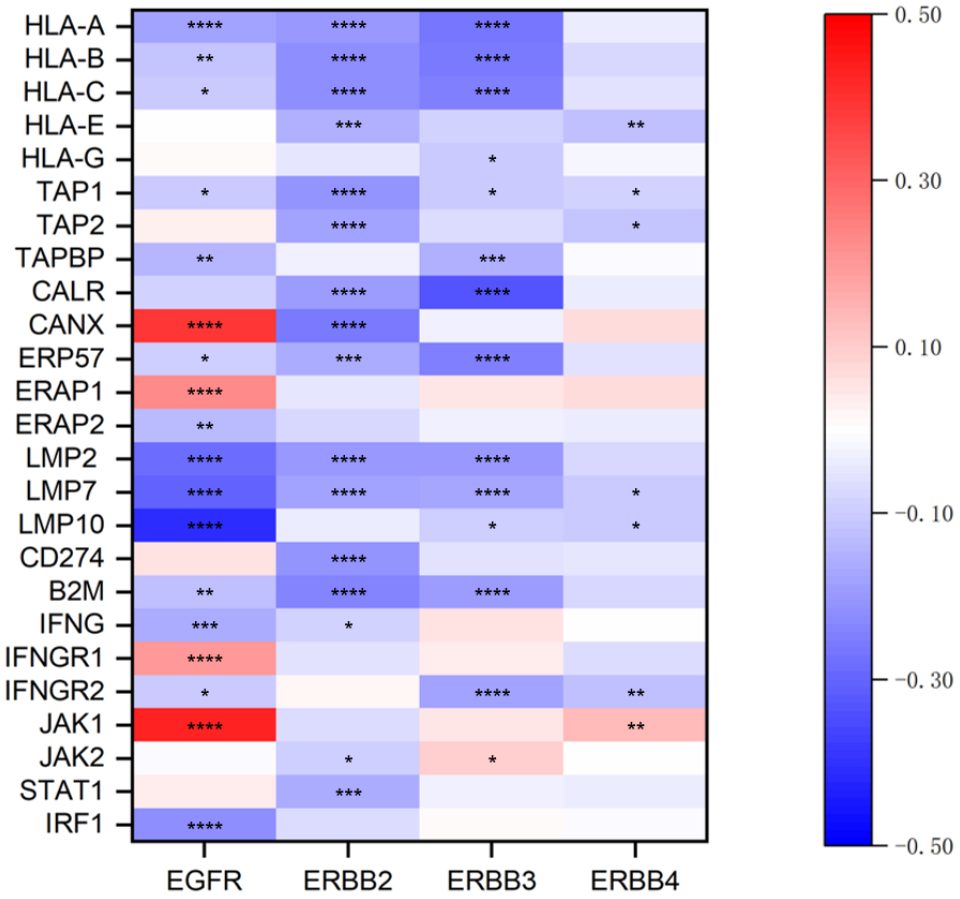

Figure 4. Correlation analysis of ERBB family members with immune relevant molecules. Gene correlation analyses were performed with the R2: Genomics Analysis and Visualization Platform (http://r2.amc.nl) and correlation statistics were shown as Pearson correlation coefficients and the heatmap generated by Origin software. Statistical significance was is given by p-values. * = p value <0.05, ** = p value < 0.01, *** = p value < 0.001, ****= p value <0.0001.

While the link to ERBB4 was weak, the other three ERBB family members showed in the majority of cases a significant negative correlation to the immune modulatory molecules. A negative correlation of EGFR, ERBB2 and ERBB3 with the expression of different HLA-I genes (HLA-A, HLA-B, and HLA-C) and the APM components TAP1, TAPBP, LMP2, LMP7, LMP10, calreticulin (CALR), ERAP2 and B2M was found. In contrast, a discordant expression between calnexin (CANX) and the ERBB family members was detected: CANX was positively associated with EGFR, but negatively with ERBB2 expression. Concerning IFN signaling components, high levels of JAK1 and IFNAR1 expression were correlated to high EGFR expression. In addition, the non-classical HLA-I molecules HLA-G and -E showed a comparable expression to EGFR, but a reduced expression in ERBB2 and ERBB3 expressing cells. Interestingly, only ERBB2 had a statistically significant negative relationship to PD-L1 expression (Figure 4).

4.2 Correlation of surface expression of ERBB family and immune relevant molecules

Based on the TCGA results demonstrating a statistically significant correlation of ERBB family members with a panel of immune related factors, EGFR, ERBB2, ERBB3, HLA-ABC and PD-L1 surface expression was determined by flow cytometry on 15 HNSCC cell lines. Interestingly, only a marginally surface expression of ERBB3 on HNSCC cell lines (data not shown) was detected, while EGFR and ERBB2 were expressed on the cell surface of all analyzed HNSCC cell lines, but to different extents. Since the expression of HLA-ABC and PD-L1, known to be involved in immune escape in HNSCC, could be modulated by oncogenic signaling and ERBB overexpression [148], the 15 HNSCC cell lines were also evaluated for the expression of HLA-ABC and PD-L1. Heterogeneous HLA-ABC expression levels were found with the high levels in PCI-1 and PCI-4B. In comparison to HLA-ABC, the PD-L1 surface levels were lower ranging between an MFI of 1.70 ± 0.53 to 63.40 ± 8.86 with the highest surface expression on UH-SCC-17A and UH-SCC-17B cells (Table 4). For further functional analysis, HNSCC cell lines relatively abundantly expressing EGFR, ERBB2 and PD-L1 were employed as models. The cell lines PCI-4B, UH-SCC-17A and UH-SCC-17B were selected for further studies.

Table 4. Distinct expression profiles of ERBB family members and immune relevant molecules in 15 HNSCC cell lines. The EGFR, ERBB2, HLA-I and PD-L1 surface expression was determined by flow cytometry as described in Materials and Methods using Ab directed against EGFR, ERBB2, HLA-ABC and PD-L1. Data represent mean ± SEM of three to five independent experiments.

	EGFR	ERBB2	HLA-ABC	PD-L1
PCI-4A	5.37 ± 1.03	6.37 ± 0.95	95.63 ± 4.73	2.90 ± 0.46
PCI-13	5.83 ± 0.85	9.13 ± 1.00	91.67 ± 3.19	2.57 ± 0.81
PCI-4B	18.67 ± 1.26	10.47 ± 1.58	223.05 ± 26.03	9.17 ± 1.62
PCI-52	8.43 ± 1.10	4.43 ± 0.90	60.73 ± 5.51	1.70 ± 0.53
SCC4	11.33 ± 1.04	11.33 ± 0.95	84.73 ± 4.55	4.37 ± 0.95
PCI-1	10.17 ± 0.76	10.70 ± 1.57	328.42 ± 62.12	3.23 ± 0.55
PCI-31	7.43 ± 0.93	8.53 ± 0.32	98.40 ± 7.11	2.87 ± 0.71
PCI-15B	32.33 ± 2.52	10.10 ± 0.30	117.17 ± 10.36	2.67 ± 0.84
PCI-30	7.93 ± 0.40	4.77 ± 0.45	146.30 ± 5.29	17.01 ± 1.55
CAL33	14.80 ± 1.71	5.63 ± 0.59	184.97 ± 25.96	24.68 ± 2.05
SAS	9.17 ± 0.76	8.93 ± 0.71	49.60 ± 6.08	19.94 ± 4.11
XF354	10.03 ± 0.50	8.07 ± 1.50	195.27 ± 25.52	8.13 ± 1.16
FADU	15.83 ± 0.76	14.43 ± 1.90	194.87 ± 3.15	3.67 ± 0.96
UH-SCC-17A	17.80 ± 6.86	10.49 ± 1.41	123.71 ± 21.11	55.68 ± 10.48
UH-SCC-17B	14.37 ± 4.07	11.53 ± 0.74	230.73 ±37.74	63.40 ± 8.86

4.3 Determination of the IC_{50} of HNSCC cell lines after treatment with lapatinib or erlotinib

To determine the effect of TKI on growth properties, lapatinib and erlotinib monotherapy for 48 hours was applied to PCI-4B, UH-SCC-17A, and UH-SCC-17B cell lines. Initial dose-response tests were conducted with each drug alone at increasing concentrations (0.001, 0.01, 0.1, 1, 10, or 100 µM) and the half-maximal inhibitory concentration (IC_{50}) values were determined. The IC_{50} values after 48hrs lapatinib treatment were calculated to be 4.861 µM, 4.436 µM and 4.508 µM, whereas the IC_{50} values upon 48hrs erlotinib treatment were calculated to be 3.135 µM, 3.585 µM and 5.433 µM in PCI-4B, UH-SCC-17A and UH-SCC-17B cell lines, respectively (Figure 5A-C)

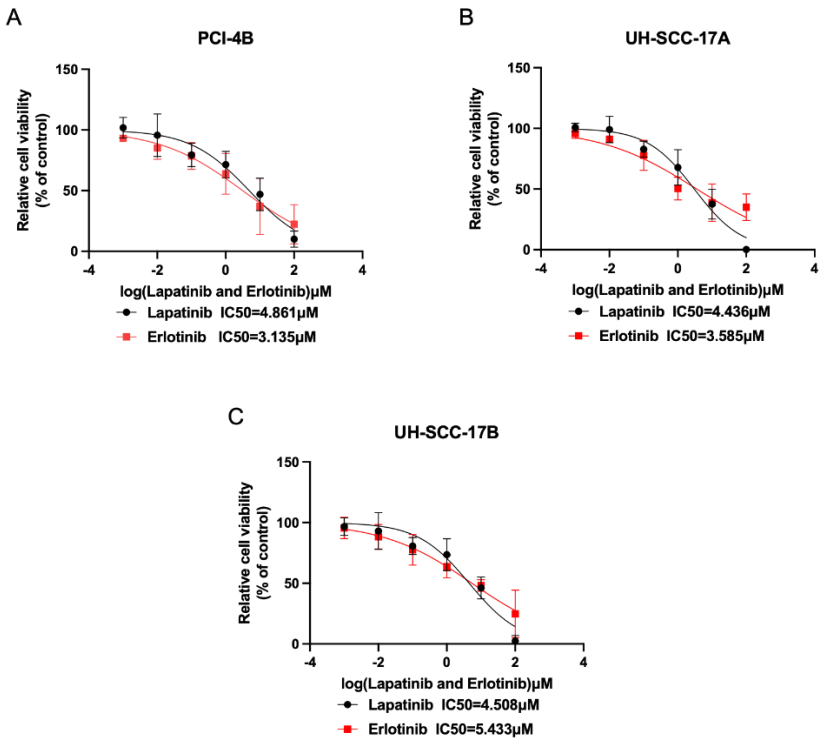

Figure 5. Distinct effects of lapatinib and erlotinib on the cell growth of HNSCC cell lines. PCI-4B (A), UH-SCC-17A(B), and UH-SCC-17B (C) cells were treated with 0.001 to 100 μM lapatinib and erlotinib for 48 hours and a XTT assay was performed to determine the effect of both inhibitors on the cell growth. Data represent mean ± SEM of three independent experiments.

4.4 Effect of lapatinib and erlotinib treatment on EGFR and ERBB2 in three HNSCC cell lines

To determine whether both TKIs influence EGFR and ERBB2 surface expression, HNSCC cell lines were left untreated or treated with lapatinib or erlotinib, before EGFR and ERBB2 surface expression was determined by flow cytometry. Lapatinib treatment significantly reduced EGFR expression in UH-SCC-17A (Figure 6B) and UH-SCC-17B (Figure 6C) cell lines, while erlotinib treatment only significantly reduced the EGFR expression in the UH-SCC-17B cell line (Figure 6C). Neither lapatinib nor erlotinib significantly altered the surface expression of ERBB2 on UH-SCC-17A and UH-SCC-17B cells. Treatment of PCI-4B cells with lapatinib or erlotinib did not significantly change EGFR and ERBB2 levels, respectively (Figure 6A).

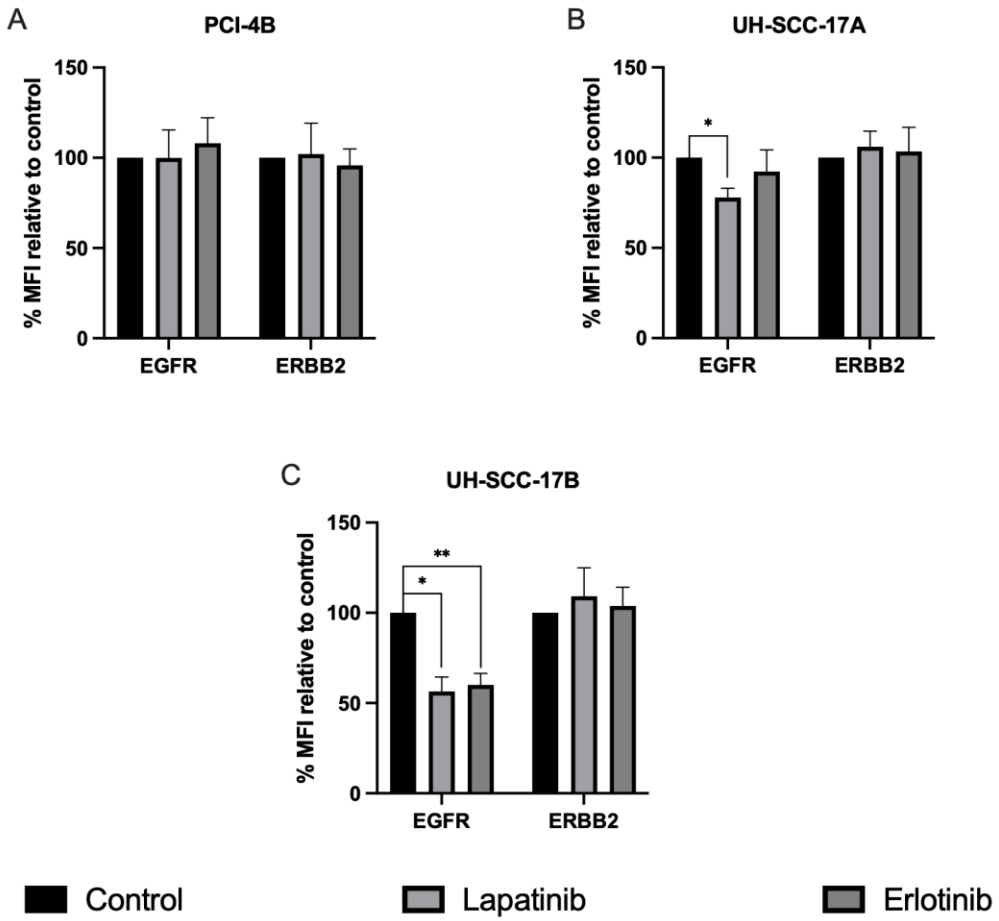

Figure 6. Effects of TKIs on the surface expression of EGFR and ERBB2 in HNSCC cell lines. The PCI-4B (A), UH-SCC-17A (B) and UH-SCC-17B (C) cell lines were left untreated or treated with IC50 lapatinib or erlotinib for 48 hours, before EGFR and ERBB2 expression was assessed by flow cytometry as described in Materials and Methods. Data represent mean ± SEM of three independent experiments. *= p value <0.05, ** = p value < 0.01.

4.5 Effects of lapatinib or erlotinib on EGFR and ERBB2 mRNA and protein expression

Since flow cytometry revealed that all three HNSCC cell lines expressed EGFR and ERBB2 (Table 4), but both TKIs had a distinct influence on their expression, their effect on EGFR and ERBB2 mRNA levels was also determined. As shown in Figure 7, lapatinib and erlotinib treatment only marginally elevated the EGFR and ERBB2 mRNA levels in PCI-4B, UH-SCC-17A and UH-SCC-17B cells suggesting no statistically significant differences between the treated and untreated groups (Figure 7A-C).

Western blot analysis was utilized to investigate the effect of lapatinib or erlotinib on the expression of basal activated expression of EGFR and ERBB2 (p-EGFR and p-ERBB2) in the HNSCC cell lines. As shown in Figure 7, an inhibition of phospho-EGFR was shown, which was more pronounced in the lapatinib-treated group compared to the erlotinib-treated group

(Figure 7D-F), while lapatinib or erlotinib treatment did not alter the protein expression levels of the HNSCC cell lines analyzed.

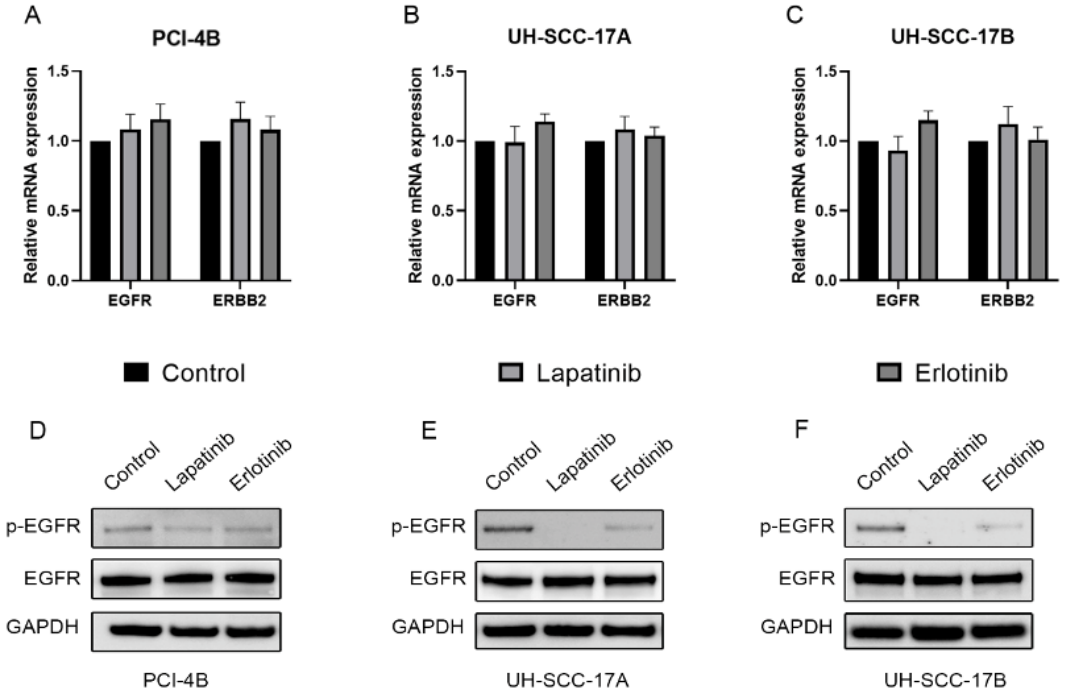

Figure 7. Effect of lapatinib and erlotinib treatment on the mRNA and protein expression of ERBB family members. The PCI-4B, UH-SCC-17A and UH-SCC-17B cells were exposed to lapatinib or erlotinib and treated for the time point indicated. The mRNA expression of EGFR and ERBB2 (A-C) was determined by RT-PCR, EGFR protein expression (D-F) by Western blot analysis as described in Materials and Methods. Staining of the Western blot with an anti-GAPDH mAb served as loading control. The flow cytometry results are provided as a percentage of MFI compared to the control group. Data represent mean ± SEM of three independent experiments. The EGFR protein was detected at molecular weight of 170-KD.

4.6 Effects of lapatinib and erlotinib on the expression of HLA-ABC and PD-L1

In the next step the effect of EGFR signaling on HLA-ABC and PD-L1 expression in the selected HNSCC cell lines was analyzed. As shown in Figure 8, both TKIs had partially distinct effects on the expression of HLA-I and PD-L1. Erlotinib treatment enhanced HLA-ABC expression and decreased PD-L1 expression in PCI-4B, UH-SCC-17A and UH-SCC-17B cells. In contrast, treatment with lapatinib lowered the surface expression of both HLA-ABC and PD-L1 in all three HNSCC cell lines as shown by flow cytometric analysis (Figure 8A-C).

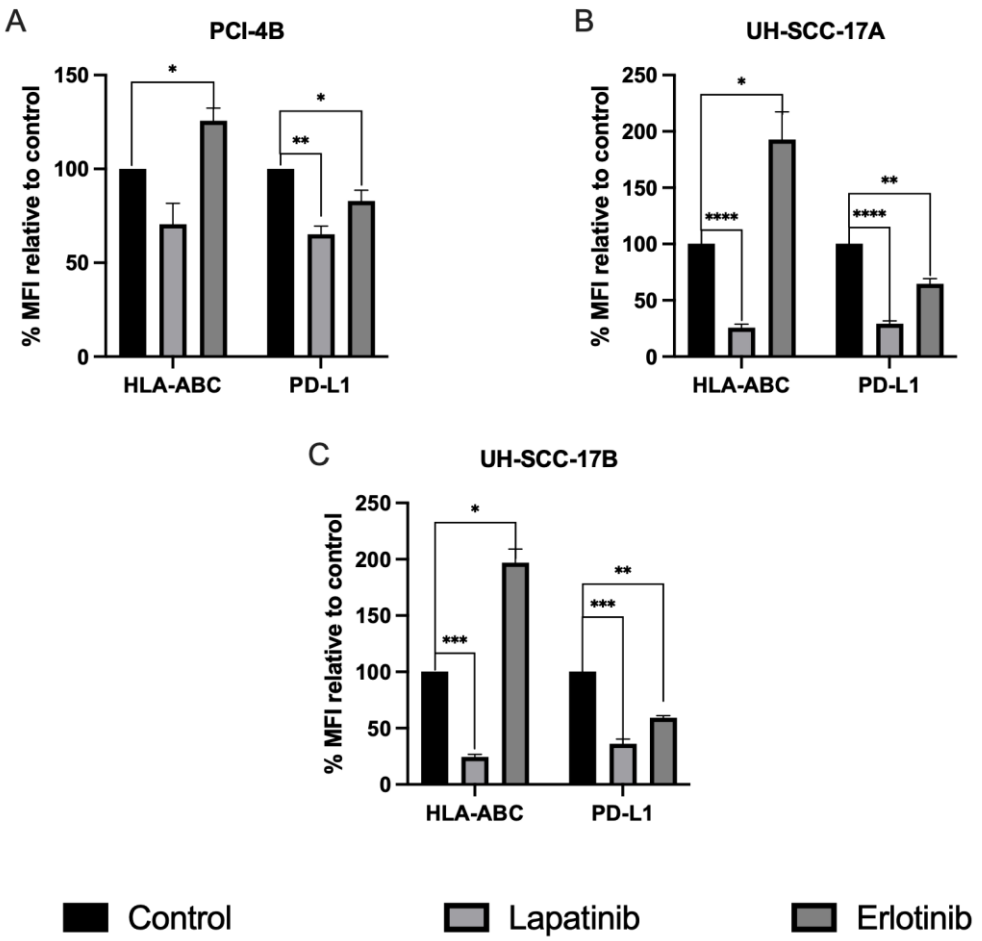

Figure 8. Modulation of HLA-ABC and PD-L1 surface expression by TKIs in HNSCC cell lines. PCI-4B, UH-SCC-17A and UH-SCC-17B cells were treated with or without lapatinib or erlotinib for 48h, before the cells were analyzed for the expression of HLA-ABC and PD-L1 by flow cytometry. The results are provided as a percentage of MFI compared to the control group. Data represent mean ± SEM of three independent experiments. * = p value <0.05, ** = p value < 0.01, *** = p value < 0.001, ****= p value <0.0001.

qPCR was then used to detect the mRNA expression levels of HLA-ABC and PD-L1 upon the TKI treatment compared to the untreated control groups. Both lapatinib and erlotinib therapy increased HLA-ABC mRNA levels in PCI-4B, UH-SCC-17A, and UH-SCC-17B cell lines relative to the control group and decreased PD-L1 mRNA levels in PCI-4B (Figure 9A), UH-SCC-17A (Figure 9B) and UH-SCC-17B (Figure 9C) cell lines.

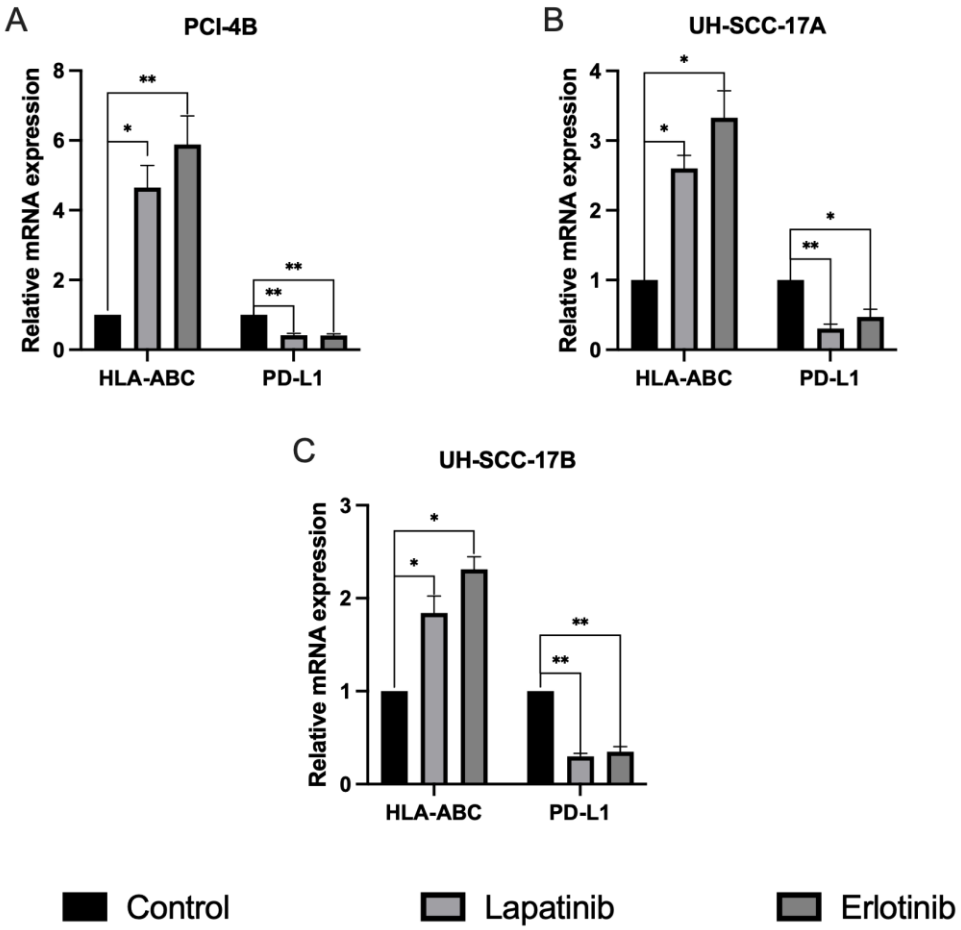

Figure 9. Effect of lapatinib and erlotinib on HNSCC cell lines. The mRNA expression levels of HLA-ABC and PD-L1 were determined in PCI-4B(A), UH-SCC-17A(B), and UH-SCC-17B (C) HNSCC cells after lapatinib or erlotinib treatment. Data represent mean ± SEM of three independent experiments. The mRNA levels of respective untreated cells served as controls and were set to "1". * = p value <0.05, ** = p value < 0.01.

4.7 Differential effect of lapatinib and erlotinib on ERBB signaling in correlation to HLA-I heavy chain

The effects of lapatinib and erlotinib treatment on ERBB signaling pathways were determined in HNSCC cell lines. As shown in Figure 10, lapatinib strongly decreased AKT and ERK phosphorylation in PCI-4B cells, whereas erlotinib showed no effect on phospho-AKT and phospho-ERK1/2 (Figure 10A). In contrast, both phospho-AKT and phospho-ERK1/2 was increased in UH-SCC-17A and UH-SCC-17B cell lines after treatment with erlotinib. There were no significant differences between the lapatinib treatment group and the control group (Figure 10B-C). Remarkably, phospho-EGFR remained suppressed after 48h of therapy (Figure 7D-F), while its downstream effectors, including phospho-AKT and phospho-ERK1/2, were elevated in UH-SCC-17A and UH-SCC-17B cell lines (Figure 10B-C). These findings imply that treating HNSCC cells with EGFR inhibitors suppresses EGFR and its downstream signaling in

PCI-4B. While in UH-SCC-17A and UH-SCC-17B cells, treatment with EGFR inhibitors increased their downstream effectors indicating the existence of other pathways implicated in the activation of AKT and ERK.

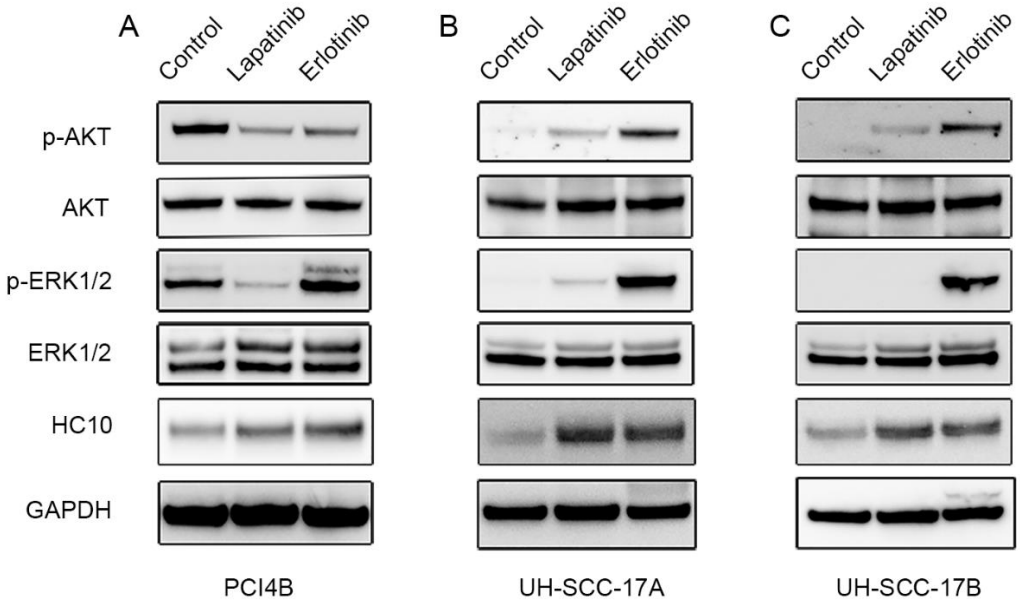

Figure 10. Effect of lapatinib and erlotinib on EGFR signal transduction and HLA-I. Western blot analysis of PCI-4B, UH-SCC-17A and UH-SCC-17B HNSCC cell lines was performed as described in Materials and Methods. Briefly, protein extracts were subjected to WB analysis using HC10, phospho-AKT/AKT, and phospho-ERK/ERK mAbs. Staining with the anti-GAPDH mAb served as control.

4.8 Effects of lapatinib and erlotinib on the TGFβ family members in HNSCC cell lines

After treatment of UH-SCC-17A and UH-SCC-17B cell lines with lapatinib and erlotinib, the expression of phosphorylated AKT and phosphorylated ERK was up-regulated, which is consistent with the observation that TKIs can affect the phosphorylation of downstream AKT and ERK by inhibiting the expression of EGFR [149, 150]. Since the TGFβ family members may be implicated in the regulation of AKT and ERK signaling pathways in the development of cancers [151], the differences between the treatment and control groups in the mRNA expression levels of the TGFβ ligands TGFβ, TGFβ2 and TGFβ3 and its receptor family members (TGFβR1, R2, R3) was examined.

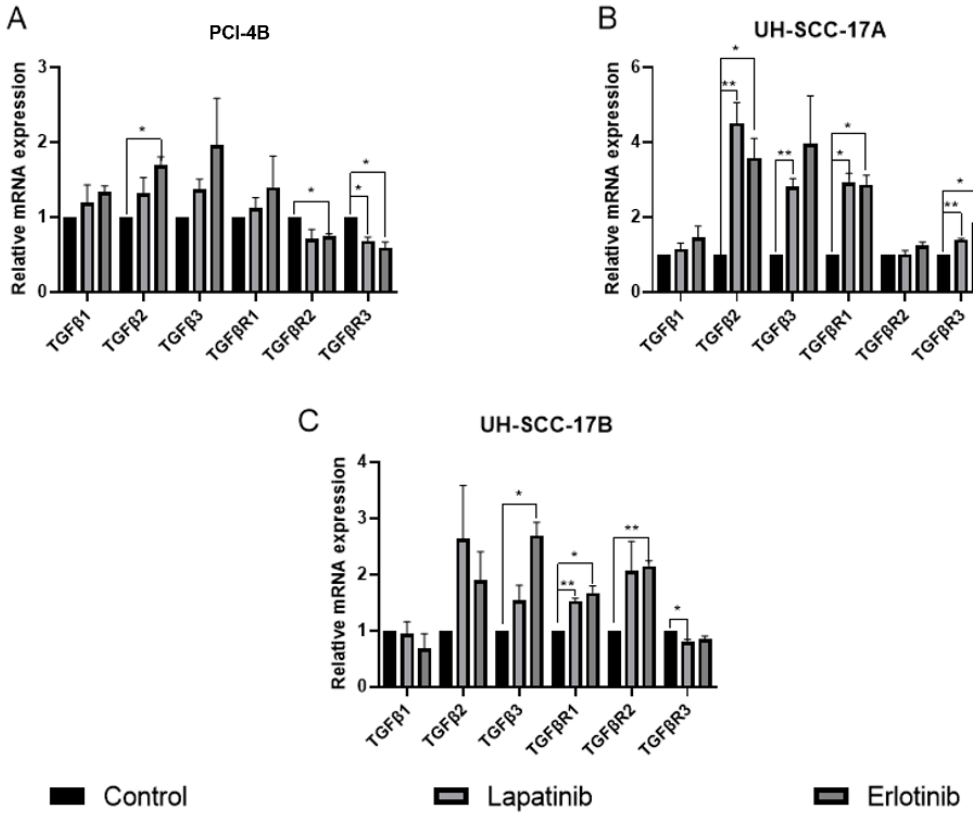

Figure 11. The mRNA expression of TGFβ family members in PCI-4B (A), UH-SCC-17A (B) and UH-SCC-17B (C). HNSCC cells left untreated or treated with lapatinib or erlotinib, before qRT-PCR was performed as described in Materials and Methods. The mRNA levels of respective untreated cells served as controls and were set to "1". Data represent mean ± SEM of three independent experiments. * = p value <0.05, ** = p value < 0.01.

After therapy with lapatinib and erlotinib, the expression of TGFβ1 and its receptor was elevated in the PIC-4B cell line, while the TGFβR2 and TGFβR3 transcription was downregulated (Figure 11A). Lapatinib and erlotinib treatment inhibited TGFβR3 mRNA expression in UH-SCC-17B cell line, while the mRNA expression of almost all TGFβ family members was upregulated (Figure 11B-C), which may contribute to the increased AKT and ERK phosphorylation levels in SCC-17A and UH-SCC-17B cell lines after lapatinib or erlotinib treatment.

4.9 TCGA public database distribution study of 22 immune cell types

Based on the differential expression of EGFR and TGFβ family members in the lapatinib or erlotinib treated cell lines versus the untreated control group, and the upon altered expression of HLA-ABC and PD-L1, known to be associated with immune cell responses, the TCGA database was used to evaluate the composition of 22 immune cell types in HNSCC

samples. The gene expression profile dataset for HNSCC obtained from UCSC XENA and the CIBERSORT algorithm was used to analyze the frequency of 22 immune cell subpopulations defined by specific markers within the dataset as well as the expression differences between normal controls and cancer patients.

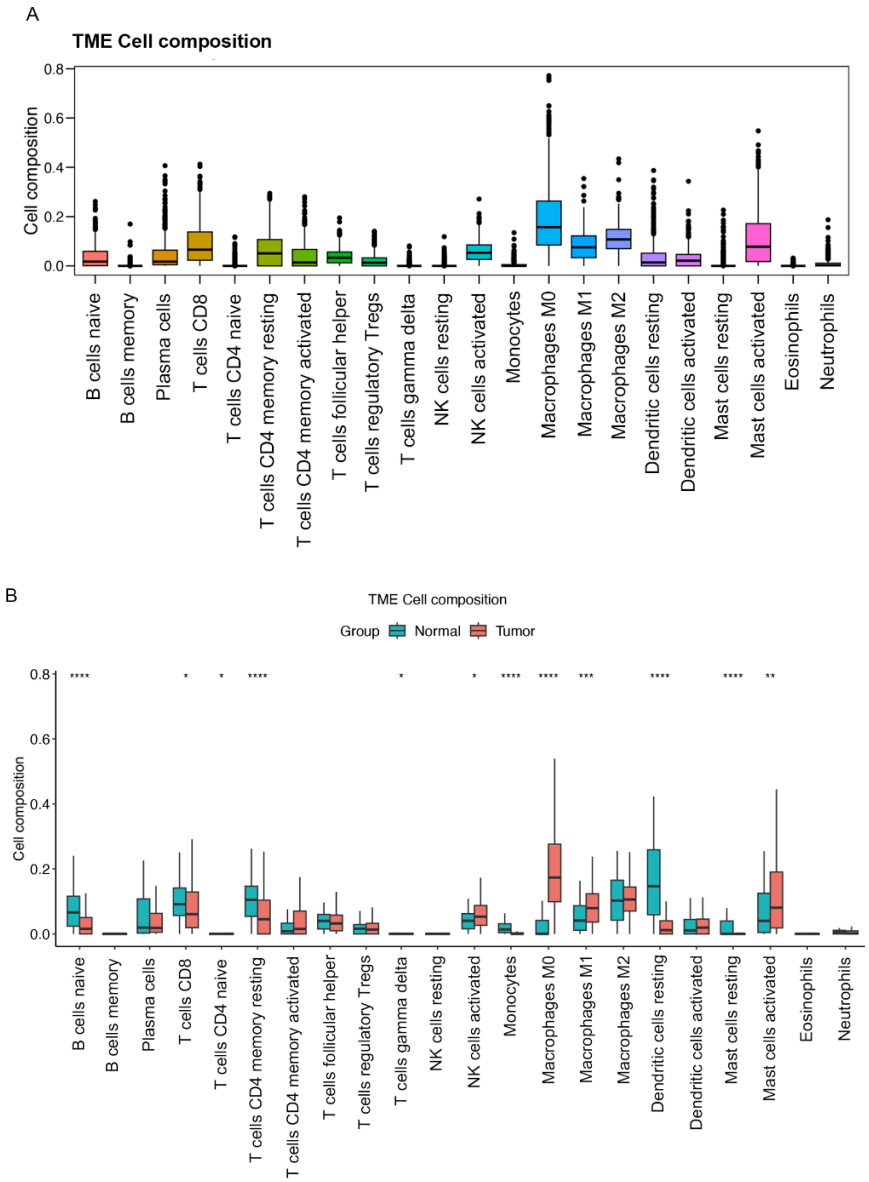

Figure 12. Composition of the immune cell repertoire in HNSCC. The immune cell composition was determined using the HNSCC TCGA datasets. The results were generated using the CIBERSORT algorithm and LM22 immune cell gene features (marker genes for 22 immune cells, downloaded from the official Cibersort website). The histograms were created by R studio. (A) General immune cell composition, (B) Differences in the frequency of immune cells between normal non-malignant tissues (n=44) and patients with HNSCC (n=502). * = p value <0.05, ** = p value < 0.01, *** = p value < 0.001, ****= p value <0.0001.

Figure 12A shows the prevalence of 22 different immune cell types in the tumor tissue from HNSCC demonstrating that immune cell subpopulation, e.g. B cells, T cells and macrophages are prevalent with in particular a high number of macrophages. Figure 12B compares the frequency of these 22 immune cells in HNSCC and non-malignant control tissues. HNSCC lesions displayed different numbers of initial B cells, $CD4^+$ T cells, NK cells, $CD8^+$ T cells, dendritic cells, macrophages (M0 and M1 subtypes) and mast cells than normal control tissues: In normal controls, the numbers of naive B cells, resting memory $CD4^+$ T cells, and $CD8^+$ T cells were higher than in tumor lesions, whereas the frequency of M0 and M1 macrophages was lower. In HNSCC lesions, the abundance of M0 and M1 macrophages, activated mast cells and NK cells were statistically significant. A statistically significant decrease in the number of naive B cells, $CD8^+$ T cells, resting memory $CD4^+$ T cells and dendritic cells was detected in HNSCC lesions.

4.10 Immune cell expression in the tissues of HNSCC patients

Based on the TCGA data results, the frequency as well as the spatial distribution of B cells, T cells and macrophages was determined using multiplex immunostaining of tissue samples obtained from individuals with HNSCC. Tissue sections were acquired from the Department of Oral and Maxillofacial Diseases at the University of Helsinki and the Institute of Pathology at the Martin Luther University of Halle-Wittenberg and subjected to multiple immunostainings using antibodies identifying B cells, T cells and macrophages. First, it was examined whether the number of immune cell subpopulations were different between primary and metastatic tumors. The metastatic cancer tissue sections from Helsinki were lymph node metastases, while the metastatic sections from the Institute of Pathology at the Martin Luther University of Halle-Wittenberg were obtained from liver, lung, pleural, and bone tissue metastatic tumor specimens and were separately analyzed. In non-lymph node metastatic lesions, CD3 (T helper cells), CD163 (macrophages), Foxp3 (T regulatory cells), CD20 (B cells) and CD8 (cytotoxic T cells) were expressed at a reduced frequency than in primary tumors, where statistically significant changes were observed in CD3- and Foxp3- labeled T cells (Figure 13A-B). The numbers of CD3, CD163, Foxp3, CD20 and CD8 positive cells were higher in lymph node metastases than in primary tumors (Figure 13C-D).

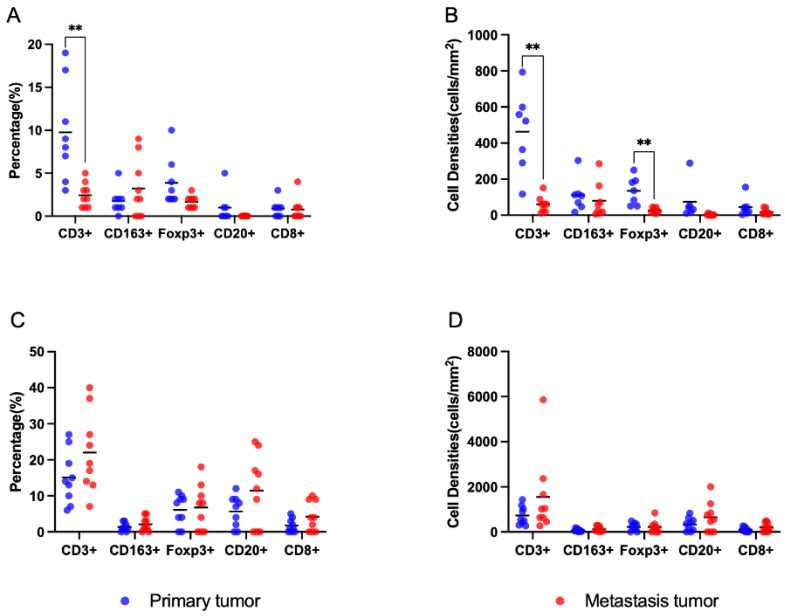

Figure 13. Percentage and density of immune-positive cells in primary and metastasis tumors. Percentage of positive cells (A) and cell density (B) in non-lymphoid metastatic tumors and percentage of positive cells (C) and cell density (D) in lymph node metastases. * = p value <0.05, ** = p value < 0.01.

In addition, the distribution of immune cell subpopulations in the central and junctional regions of the tumor sections were confirmed. According to the findings, the proportion and cell density of CD3, CD163, Foxp3, CD20 and CD8 positive cells were lower in the tumor center than in the tumor margin (Figure 14A-D).

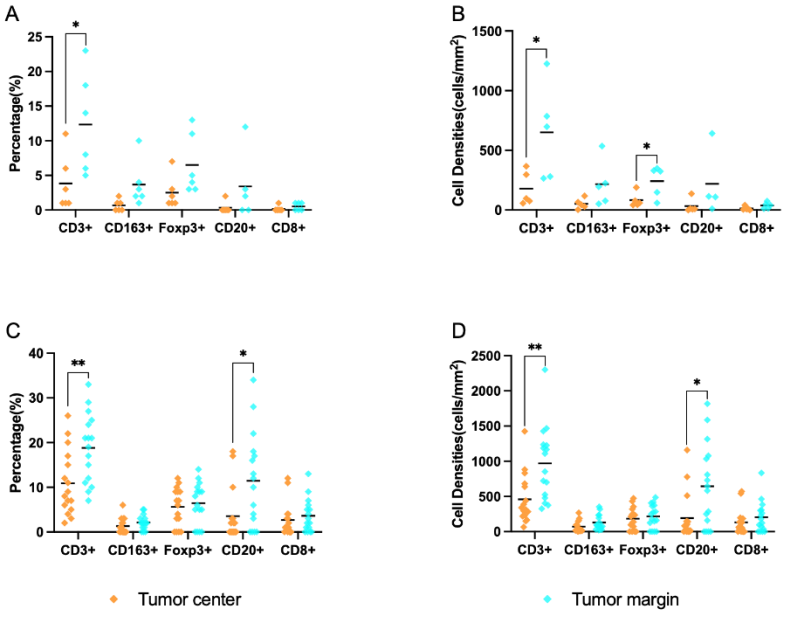

Figure 14. Percentage and density of immune-positive cells in the central region of the tumor and in the tumor junctional area. Percentage of positive cells (A) and cell density (B) in primary and non-lymphoid metastatic tumors from the Institute of Pathology, Martin Luther University of Halle-Wittenberg and percentage of positive cells (C) and cell density (D) in

primary and lymph node metastases from the University of Helsinki. * = p value <0.05, ** = p value < 0.01.

Furthermore, the number of immune cells in the specimens of HNSCC patients with a history of treatment (primarily radio-chemotherapy) and those without any history of treatment were compared. With the exception of CD163 macrophages, the numbers of the other immune cell subpopulations in the treatment group were lower than in the non-treatment group (Figure 15) indicating that radio-chemotherapy killed a large number of immune cells, while killing tumor cells.

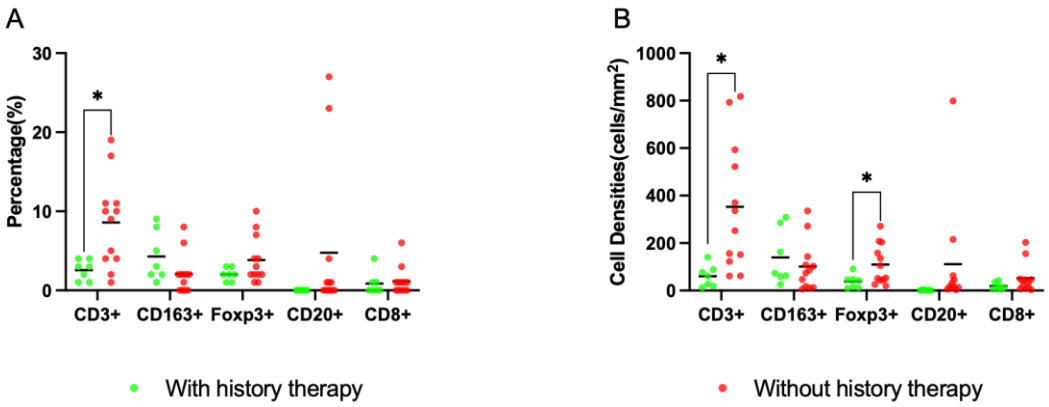

Figure 15. Percentage and density of immune cell subpopulations with and without treatment history. HNSCC lesions of patients with history treatment (A) and without history treatment (B) was analyzed by multispectral imaging as described in Material and Methods. * = p value <0.05.

4.11 The correlation of immune cell markers and chemokines

Based on the differential expression in the previous analysis of slices from patients with HNSCC, the expression of immune cell markers (CD3, CD163, Foxp3, CD20 and CD8) and various chemokines (CCL2, CCL5, CCL22, CXCL9 and CXCL10) were determined using in silico analysis of the human TCGA HNSCC dataset "Tumor Head Neck Squamous Cell Carcinoma" containing 520 samples, and their expression patterns were correlated. As depicted in Figure 16, there was a positive correlation between the genes of the immune cell markers used and the detected chemokines. Specifically, there was a strong correlation between the immune markers CD3 and CD8 and the chemokines CCL5, CXCL9, and CCL10. The correlation analysis demonstrated statistically significant differences between the immune cell markers and chemokines.

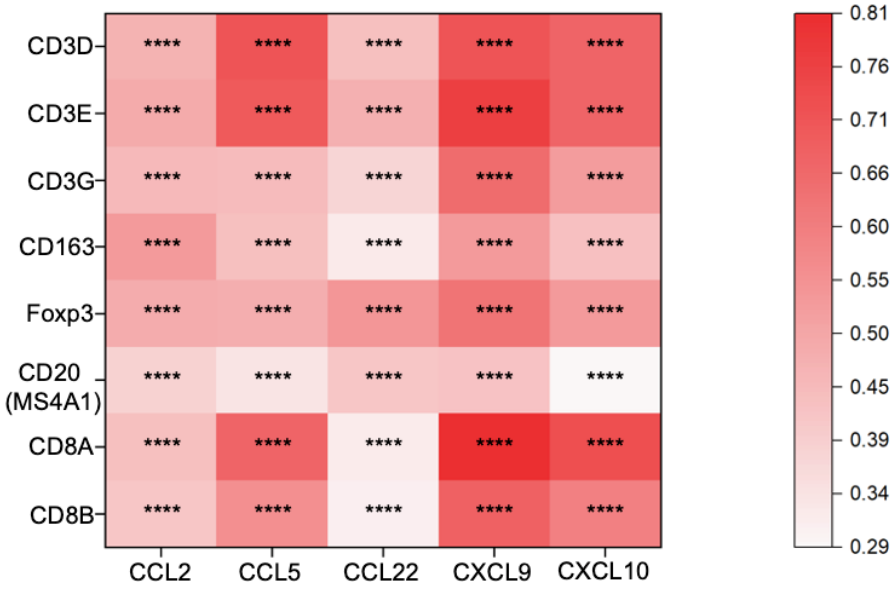

Figure 16. Correlation analysis of immune cell markers with immune relevant chemokines. Gene correlation analyses were performed with the R2: Genomics Analysis and Visualization Platform (http://r2.amc.nl) and correlation statistics were shown as Pearson correlation coefficients and the heatmap generated by Origin software. Statistical significance is given by p-values. ****= p value <0.0001.

4.12 Modulations of immune-related chemokines after treatment with lapatinib or erlotinib

Upon *in silico* analysis of public available patient databases and clinical specimens, we discovered that the immune cell repertoire and distribution composition is altered in HNSCC lesions. Using the HNSCC cell lines, the mRNA expression of immune-related chemokines, in untreated and TKI treated HNSCC cell lines was compared. After treatment with lapatinib or erlotinib, the chemokines CCL2, CCL5, CCL22, CXCL9 and CXCL10 were found to be variably elevated in these selected HNSCC cell lines with CCL5 and CXCL10 exhibiting the most dramatic alterations (Figure 17).

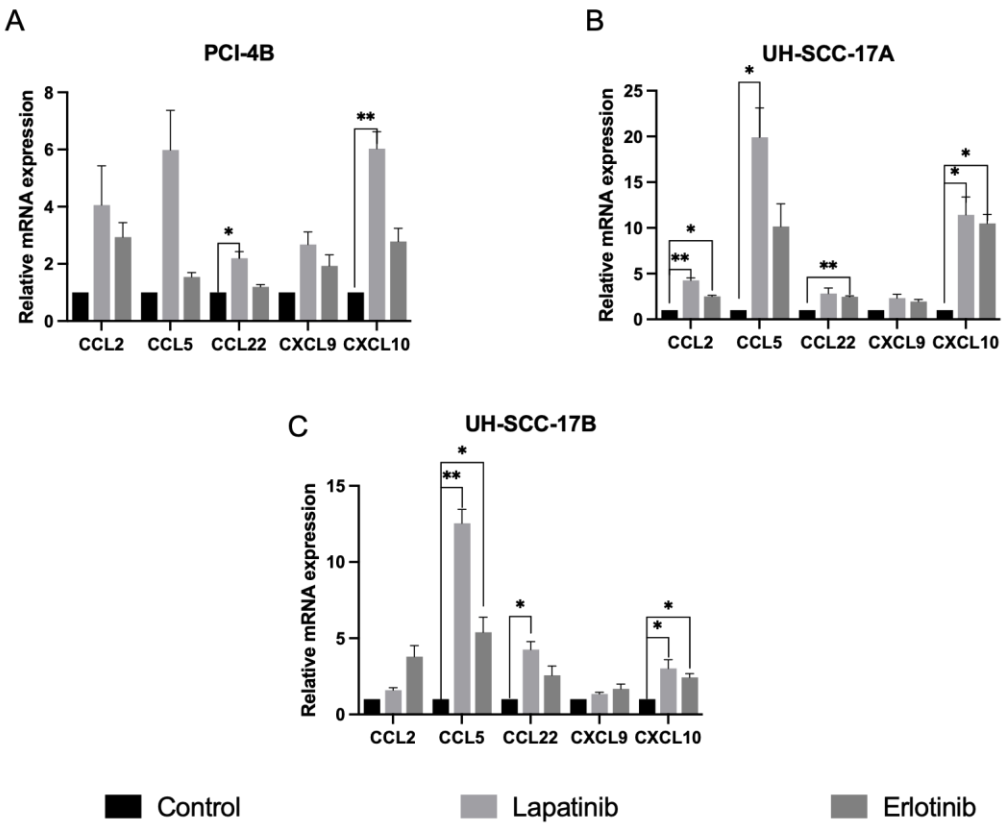

Figure 17. Effects of lapatinib or erlotinib treatment on the mRNA expression of immune-related chemokines. The mRNA expression of CCL2, CCL5, CCL22, CXCL9 and CXCL10 chemokines in PCI-4B (A), UH-SCC-17A (B) and UH-SCC-17B (C) cell lines were measured by qPCR assay. Data represent mean ± SEM of three independent experiments. *= p value <0.05, ** = p value < 0.01.

We then examined the concentration of CCL5 and CXCL10 in the supernatant of the untreated and TKI treated HNSCC cell lines using an ELISA assay. The results indicated that in UH-SCC-17A and UH-SCC-17B cell lines the CCL5 concentration was significantly increased and statistically different in the lapatinib-treated group (UH-SCC-17A: 233.47 ± 42.28 pg/mL, UH-SCC-17B: 63.13 ± 23.27 pg/mL) compared to the control group (UH-SCC-17A: 69.16 ± 17.17 pg/mL, UH-SCC-17B: 24.32 ± 16.63 pg/mL), whereas the changes were not statistically significant in the erlotinib-treated group (Figure 18A-F). CXCL10 levels was not significantly altered in all three cell lines upon treatment.

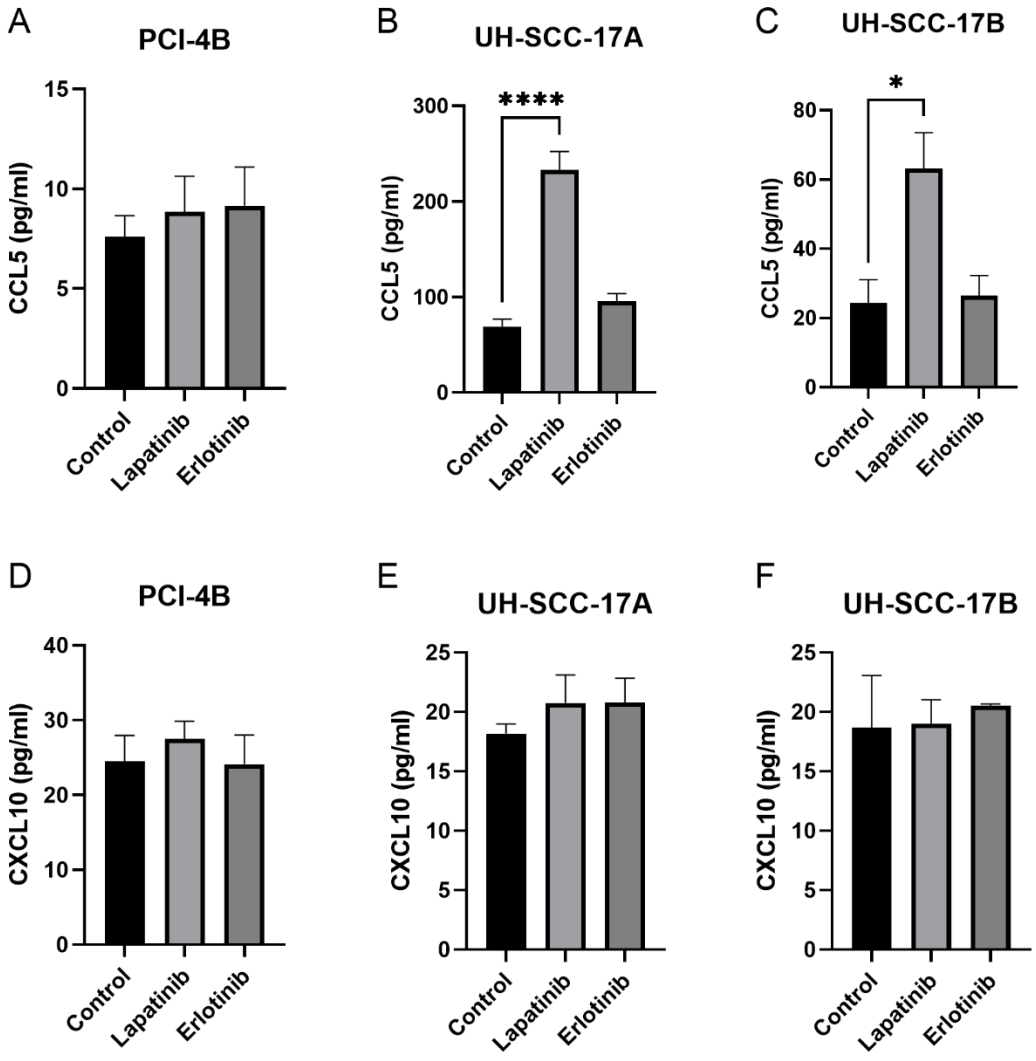

Figure 18. Effects of TKIs on the secretion of CCL5 and CXCL10into the HNSCC culture supernatant. The culture supernatant of untreated or lapatinib- or erlotinib-treated cells upon cultivation for 48 hours was collected and the concentration of CCL5 (A-C) and CXCL10 (D-F) was measured by ELISA assay. Data represent mean ± SEM of three independent experiments. *= p value <0.05, **** = p value < 0.0001.

5 Discussion

The current conventional treatment of HNSCC patients is surgery, radiotherapy, and chemotherapy have only provided short-term efficacy in some HNSCC patients leading to a high morbidity and mortality. The recent years, the implementation of targeted therapies, such as TKIs [152, 153], as well as immunotherapeutic agents have been shown an increased treatment efficacy in a limited number of recurrent and metastatic HNSCC patients, which might be at least partially associated with a high immune infiltration within the tumor [154], but the response rates need still to be improved.

RTKs have emerged as key regulators of major cellular processes, such as cell proliferation, differentiation, survival, metabolism, migration, and cell cycle control upon their activation [155] and are furthermore involved in the control of developmental processes including stem and progenitor cell generation [156]. In depth *in silico* analysis of ERBB family members and HLA-I and APM components using the HNSCC TCGA database was performed demonstrating a negative correlation of EGFR, ERBB2 and ERBB3 expression a reduced immunogenicity defined by downregulation of HLA-I and most APM components was found. This was accompanied by a reduced number of immune effector cells in HNSCC lesions. These data suggest that targeting ERBB family members may affect the immune response thereby playing an important therapeutic role beyond growth inhibition in HNSCC patients. Heterogeneous expression levels of EGFR and ERBB2 were found in 15 accessible HNSCC cell lines using flow cytometry. Some of the 15 HNSCC cell lines had significant high levels of EGFR and ERBB2 expression, while the others exhibited lower levels. This variation in the surface expression of ERB family members might explain why HNSCC patients variably respond to TKI therapy. Intracellular inhibitors of RTK signaling are also capable of regulating the diverse developmental pathways in stem and progenitor cells, which frequently determine the outcomes of RTK activation [156]. It has been discovered that elevated levels of RTKs correlate significantly with increased cancer aggressiveness, progression and poorer prognosis and disease-free survival [157]. High EGFR expression is associated with a poor prognosis in HNSCC; therefore, inhibiting aberrant activation of the EGFR signaling pathway has been a focus of research in the past [158]. In our experimental results, the TKIs lapatinib and erlotinib reduced the surface expression of EGFR on UH-SCC-17A and UH-SCC-17B tumor cells, while the effect on ERBB2 was not statistically significant. MRNA expression levels of EGFR and ERBB2 was observed in both the TKI therapy group and the control group; however, the effect of lapatinib and erlotinib on the mRNA expression of EGFR and ERBB2 was not statistically significant.

Furthermore, the phosphorylation level of EGFR was down-regulated after treatment suggesting an inhibition of EGFR activation by these inhibitors. The decreased phosphorylation levels of EGFR also affect the downstream factors AKT and ERK. Lapatinib treatment of PCI-4B cell line lowered the phosphorylation levels of AKT and ERK, while in the other two cell lines, treatment with both lapatinib and erlotinib increased the phosphorylation levels of AKT and ERK, particularly in the erlotinib treatment group. These results provide some evidence that TKIs have in some cases poor efficacy in the therapy of HNSCC patients. These results hypothesize that TKI therapy may influence additional pathways associated with AKT and ERK leading to an increase of their phosphorylation levels. In addition, it is noteworthy that treatment with lapatinib decreased the phosphorylation level of EGFR more effectively than treatment with erlotinib using the same therapeutic concentration of IC_{50}. In comparison to the erlotinib treatment group, the capacity of lapatinib to lower the level of phosphorylation of AKT and ERK was shown to be much lower. This may be because lapatinib is an inhibitor of both EGFR and ERBB2, while erlotinib only inhibits EGFR [49]. Lapatinib appears ineffective in EGFR inhibitor-naive or refractory patients with recurrent/metastatic head and neck squamous cell carcinoma as a single agent, despite being well tolerated [159, 160]. Erlotinib is safe for long-term use and demonstrates a potential survival advantage compared to historical controls [161, 162]. Combined with the results of EGFR and its downstream AKT and ERK factors after lapatinib or erlotinib treatment, TKIs treatment of UH-SCC-17A and UH-SCC-17B cell lines led to an upregulation of the downstream EGFR pathways AKT and ERK, which illustrates the limitations of lapatinib or erlotinib treatment.

TGFβ signal transduction shields tumor cells from targeted therapy by elevating the expression of EGFR, ERK, and AKT, which may be a crucial element in chemotherapy, targeted therapy and immunotherapy resistance [151]. TKI treatment of UH-SCC-17A and UH-SCC-17B cell lines increased the mRNA levels of nearly all members of the TGFβ family. According to the reported data, an increase in the phosphorylation of AKT and ERK may be accompanied by an increased TGFβ expression. Since lapatinib is a dual inhibitor of EGFR and ERBB2, the expression levels of phosphorylated AKT and ERK might be significantly higher in UH-SCC-17A and UH-SCC-17B after treatment with erlotinib than with lapatinib. In the PCI-4B cell line, TGFβR2 and TGFβR3 mRNA levels were decreased in the treatment group compared to the control group, the remaining TGFβ members were elevated to a lesser extent than in UH-SCC-17A and UH-SCC-17B. These data suggest that phosphorylation of EGFR, AKT and ERK was

inhibited in the PCI-4B cell line, which may be related to the altered regulation TGFβ TGFβ family members, which has to be confirmed by other studies.

HLA-I plays a crucial role in immune defense by providing antigens to T lymphocytes [163], which then lead to the initiation of adaptive immune responses in many pathological situations, such as during autoimmunity, cancer, and infection. By altering or downregulating HLA- I or its interactants, tumor cells inhibit the activation signal to T cells thereby evading the immune system [164-166]. Many hematopoietic cells, including dendritic cells and lymphocytes, express relatively high numbers of HLA-I APM components and as a result have significant levels of HLA-I antigens on cell surfaces under baseline conditions [167, 168]. In contrast, the majority of HNSCC cells have low expression patterns of APM components and lower levels of HLA-I on their cell surface under basal conditions. A large number of distinct types of human cancer have been reported to lose or have a reduced HLA-I surface expression to varying degrees[169, 170]. A low HLA-I phenotype has been observed in many of the most prevalent human cancers, including HNSCC [148, 169]. Cancers may not be homogenous, and the expression of HLA-I in their cells and/or distinct regions may vary. Moreover, expression may change as the cancer progresses and may differ between primary and metastatic sites [104, 171]. Indeed, highly heterogeneous HLA-I expression levels were found in the HNSCC cell lines analyzed. Interestingly, erlotinib can successfully upregulate the expression levels of HLA-ABC in the three HNSCC cell lines selected for functional studies. Unexpectedly, after treatment with lapatinib the expression of HLA-ABC on the surface of all three HNSCC cell lines was reduced. Similar modifications have also been observed in breast cancer cell lines treated with lapatinib suggesting the induction of other regulatory elements [172]. Flow cytometry revealed that only the expression of HLA-ABC was reduced following treatment with lapatinib, while all other protein and mRNA levels were up-regulated, and the mRNA and protein levels of HLA-ABC were similarly up-regulated after treatment with erlotinib. In conclusion, both lapatinib and erlotinib can successfully up-regulate the expression of HLA-ABC suggesting a dual role of both TKIs in the treatment by inhibiting the growth and promoting the immunogenicity of HNSCC cells.

PD-L1 is an essential immune checkpoint protein that binds to PD-1 on T lymphocytes [173] thereby negatively interfering with T cell responses [174, 175]. Multiple cancer types express elevated levels of PD-L1 and use PD-L1/PD-1 signaling to evade T cell immunity [175]. Based on the successful implementation of anti-PD-1/PD-L1 antibodies in many cancer types, PD-L1

has become an essential protein in immuno-oncology, and its function and regulatory mechanism are being intensively studied. Since PD-L1 plays a crucial role in promoting tumor immune escape, PD-L1 was chosen as an important indicator of the immunogenicity and the effect of TKIs on this molecule. The results of flow cytometry showed that PD-L1 on the cell surface of the UH-SCC-17A and UH-SCC-17B cell lines was at the highest when compared to that of the 15 HNSCC cell lines. Surface PD-L1 expression and PD-L1 mRNA expression were both shown to be down-regulated in HNSCC cells after treatment with lapatinib and erlotinib. These data suggest that the TKI treatment may be able to revert the immune escape of HNSCC.

A comprehensive overview of the TME in HNSCC is useful for discovering new ways to treat HNSCC or modifying the TME to improve immunotherapy's efficacy. Numerous studies [176-178] have demonstrated that a dense infiltration of T cells, particularly cytotoxic $CD8^+$ T cells, is indicative of a favorable prognosis, which has been shown in breast, bladder, ovarian, gastric, prostate cancers and HNSCC [177, 179-181]. In the majority of tumors, M2 macrophages are the predominant macrophage subtype associated with chronic inflammation, which promotes tumor growth and the development of an aggressive phenotype. In contrast, a high density of M1 macrophages may indicate a favorable prognosis in patients with NSCLC, hepatocellular carcinoma (HCC), ovarian or gastric cancer [182]. Previous research on immune-related markers HLA-ABC and PD-L1, ERBB family members EGFR and ERBB2, and TGFβ family members suggested that the immune response plays a significant role in HNSCC cells. To further clarify the role of immune cells in HNSCC, a TCGA dataset of HNSCC was analyzed regarding their immune cell repertoire demonstrating a significant number of T cells and macrophages. Primary tumor tissues and metastatic lesions obtained from lymph node, bone, liver, pleura and lung were analyzed using multiple staining and the frequency of B cells, T cells and macrophages was compared in primary lesions and metastasis. Immune cell analysis revealed that lymph node metastases expressed more immune cells than non-lymph node metastases, possibly related to the presence of large number of immune cells in lymph node metastases. The difference between the level of immune cells expressed in metastases and primary tumors further illustrates the important role of immune response in the progression of HNSCC. We also analyzed the difference between immune cells in the tumor center and the tumor margin and found that the expression of immune cells in the tumor center was lower than that in the tumor margin. This suggests that for solid tumors, such as HNSCC, it is difficult for immune cells to reach the central region of the tumor, which highlights a significant difficulty with current squamous cell carcinoma treatments. We also analyzed slices with and

without treatment history at the same time and found that the number of T cells and B cells in the tissues of HNSCC patients who had history treatment (mainly radio(chemo)therapy) was lower than those of patients without treatment history. These data indicate that radio(chemo)therapy is likewise highly cytotoxic towards immune cells, which is not conducive to the immune system's suppression of tumor cells.

One task of chemokines is to promote tumor immunity, since immune cells with anti-tumor efficacy can be recruited into the tumor microenvironment (TME) through the chemokine and chemokine receptor signaling pathway [33]. Treatment with TKIs increased the expression of HLA-I, which is involved in regulation of the immune response as well as the mRNA expression of TGFβ family members, which have been demonstrated to influence the biological functions of immune cells [183]. The expression of PD-L1, which is involved in the immune evasion of tumor cells, was decreased after treatment with TKI therapy. CCL2 and CCL20 are known to inhibit the anticancer immune response by attracting macrophages, neutrophils, and MDSCs into the tumor microenvironment (TME) [184-186]. Higher CCL5, CXCL9 and CXCL10 levels following panitumumab treatment stimulate the migration of $CD8^+$ T cells, suggesting that targeting EGFR could modify the TME and hence improve tumor control by ICIs. EGFR signaling lowered CXCL10 and CCL5 production, hence decreasing $CD8^+$ T cell infiltration in EGFR-mutated lung adenocarcinoma [187]. The production of tumor-derived CCL5, CXCL9 and CXCL10 was correlated with tumor-infiltrating lymphocytes in melanoma [188], and the same chemokine profile was correlated with $CD8^+$ T cell infiltration in solid tumors [189, 190]. In the database of HNSCC patients, immune cell marker genes (CD3, CD163, Foxp3, CD20 and CD8) were positively correlated with chemokines (CCL2, CCL5, CCL22, CXCL9 and CXCL10) and statistically distinct, whereas mRNA results for macrophage and T cell-associated chemokines in the treated and untreated groups indicated that these cytokines were differentially upregulated after lapatinib or erlotinib treatment. The chemokines CCL5 and CXCL10 were selected for further analysis in the supernatant of HNSCC cell lines left untreated or treated with TKIs. The results showed that CCL5 was significantly higher in the lapatinib-treated group than in the control group. These data suggest that $CD8^+$ T cells and macrophages may play an important role in tumor development as well as in the treatment process and deserve further study.

In conclusion, comparison of the tumor center and tumor margin of primary and metastatic HNSCC tissue sections revealed differences in the frequency of B cells, T cells and

macrophages suggesting the importance of immune cells in carcinogenesis and progression. The EGFR inhibitors lapatinib and erlotinib significantly increased HLA-ABC expression and decreased PD-L1 expression, while reducing EGFR phosphorylation. The mRNA levels of immune cell-associated chemokines were upregulated after TKI treatment indicating the feasibility of immunotherapy in HNSCC. In HNSCC cell lines, TKI drugs did not inhibit the AKT and ERK pathways as expected. Although TKI inhibitors were able to reduce the phosphorylation levels of EGFR in some HNSCC cell lines, they were unable to downregulate the phosphorylation levels of AKT and ERK; some other pathways may be involved in regulating the expression of AKT and ERK. The results demonstrated that TKI elevated the mRNA levels of the majority of the TGFβ family members and that the TGFβ signaling pathway may be implicated in the upregulation of AKT and ERK phosphorylation levels, which requires further study. Similarly, different HNSCC cell lines may respond differently to the same treatment. There is a high degree of similarity between the primary and metastatic tumor cell lines tested in this experiment; however, when comparing primary and metastatic tumor tissue samples, there are substantial differences in immune cells; therefore, additional experimental evidence is required to determine whether primary and metastasis tumors share similarities.

6 Summary

HNSCC has a high global mortality rate and current treatment options have not improved the prognosis of patients. According to recent findings, immunosuppressive therapy may be a novel study approach. The EGFR inhibitors lapatinib and erlotinib may play an essential role in the therapy of HNSCC, although their present clinical efficacy in the treatment of HNSCC patients is unsatisfactory. This work demonstrated that lapatinib or erlotinib could effectively block EGFR phosphorylation, and we further investigated the expression changes of AKT and ERK downstream of EGFR. We discovered that lapatinib inhibits the phosphorylation of AKT and ERK in PCI-4B cells more efficiently than erlotinib, thereby preventing tumor development. In other HNSCC cell lines, EGFR inhibitors did not significantly suppress AKT and ERK pathways, but rather increased their phosphorylation levels, indicating that additional pathways including EGFR-related pathways are also involved in the regulation of AKT and ERK activation. Upregulation of TGFβ and its receptors can activate EGFR-dependent AKT and ERK signaling pathways, indicating that TKI and TGFβ inhibitors are effective against cancer. The TKI chemical may influence TGFβ signaling in addition to inhibiting EGFR and its downstream signaling pathways. Some additional signaling pathways may also contribute to the process; the ultimate manifestation of AKT and ERK may involve the coordination of several pathways. As an immunosuppressive factor, higher expression of PD-L1 is related to increased tumor invasiveness and mortality, and investigations have shown that EGFR inhibitors can reduce PD-L1 expression. HLA-ABC participates in the presentation of antigen molecules during cellular immunity and plays a crucial function in the body's anti-tumor immunological response. We discovered that TKI inhibitors could upregulate HLA-ABC expression. Simultaneously, the response of primary and metastatic HNSCC cell lines to lapatinib and erlotinib was more consistent; however, there were still differences in the expression levels of some components, which required further investigations. Simultaneously, multiple immunostaining analyses of clinical HNSCC patient sections revealed differences in common immune cells between HNSCC primary tumor and metastatic tumor samples, tumor neutral and tumor junction regions, and with or without treatment history. In combination with the effects of TKI treatment on immune-related factors and immune chemokines in HNSCC cell lines, this demonstrates the viability of immunotherapy for HNSCC. In conclusion, the response of HNSCC cell lines to TKIs is a

result of multiple signaling pathways, and immunotherapy and multi-target combination therapy may represent a new treatment strategy for HNSCC.

7 Reference

1. Bray, F., et al., The ever-increasing importance of cancer as a leading cause of premature death worldwide. Cancer, 2021. **127**(16): p. 3029-3030.
2. Mody, M.D., et al., Head and neck cancer. Lancet, 2021. **398**(10318): p. 2289-2299.
3. Wyss, A., et al., Cigarette, cigar, and pipe smoking and the risk of head and neck cancers: pooled analysis in the International Head and Neck Cancer Epidemiology Consortium. Am J Epidemiol, 2013. **178**(5): p. 679-90.
4. Hashibe, M., et al., Alcohol drinking in never users of tobacco, cigarette smoking in never drinkers, and the risk of head and neck cancer: pooled analysis in the International Head and Neck Cancer Epidemiology Consortium. J Natl Cancer Inst, 2007. **99**(10): p. 777-89.
5. Mehanna, H., et al., Prevalence of human papillomavirus in oropharyngeal and nonoropharyngeal head and neck cancer--systematic review and meta-analysis of trends by time and region. Head Neck, 2013. **35**(5): p. 747-55.
6. Yete, S., W. D'Souza, and D. Saranath, High-Risk Human Papillomavirus in Oral Cancer: Clinical Implications. Oncology, 2018. **94**(3): p. 133-141.
7. Shah, A., et al., Oral sex and human papilloma virus-related head and neck squamous cell cancer: a review of the literature. Postgrad Med J, 2017. **93**(1105): p. 704-709.
8. Blanco, R., et al., High-Risk Human Papillomavirus and Epstein-Barr Virus Coinfection: A Potential Role in Head and Neck Carcinogenesis. Biology (Basel), 2021. **10**(12).
9. Copper, M.P., et al., Role of genetic factors in the etiology of squamous cell carcinoma of the head and neck. Arch Otolaryngol Head Neck Surg, 1995. **121**(2): p. 157-60.
10. Vageli, D.P., et al., Bile reflux and hypopharyngeal cancer (Review). Oncol Rep, 2021. **46**(5).
11. Li, X., et al., Fat mass and obesity-associated protein regulates arecoline-exposed oral cancer immune response through programmed cell death-ligand 1. Cancer Sci, 2022. **113**(9): p. 2962-2973.
12. Hashibe, M., et al., Epidemiologic review of marijuana use and cancer risk. Alcohol, 2005. **35**(3): p. 265-75.
13. Levi, F., et al., Food groups and risk of oral and pharyngeal cancer. Int J Cancer, 1998. **77**(5): p. 705-9.
14. Sturgis, E.M. and K.B. Pytynia, After the smoke clears: environmental and occupational risks for carcinoma of the upper aerodigestive tract. Cancer J, 2005. **11**(2): p. 96-103.
15. Saku, T., et al., Salivary gland tumors among atomic bomb survivors, 1950-1987. Cancer, 1997. **79**(8): p. 1465-75.
16. Wang, H., et al., Immune Checkpoint Inhibitor Toxicity in Head and Neck Cancer: From Identification to Management. Front Pharmacol, 2019. **10**: p. 1254.

17. Kitamura, N., et al., Current Trends and Future Prospects of Molecular Targeted Therapy in Head and Neck Squamous Cell Carcinoma. Int J Mol Sci, 2020. **22**(1).

18. Canning, M., et al., Heterogeneity of the Head and Neck Squamous Cell Carcinoma Immune Landscape and Its Impact on Immunotherapy. Front Cell Dev Biol, 2019. **7**: p. 52.

19. Chen, S.M.Y., et al., Tumor immune microenvironment in head and neck cancers. Mol Carcinog, 2020. **59**(7): p. 766-774.

20. Curry, J.M., et al., Tumor microenvironment in head and neck squamous cell carcinoma. Semin Oncol, 2014. **41**(2): p. 217-34.

21. Hadrup, S., M. Donia, and P. Thor Straten, Effector CD4 and CD8 T cells and their role in the tumor microenvironment. Cancer Microenviron, 2013. **6**(2): p. 123-33.

22. Park, Y.J., et al., Tumor microenvironmental conversion of natural killer cells into myeloid-derived suppressor cells. Cancer Res, 2013. **73**(18): p. 5669-81.

23. Umansky, V. and A. Sevko, Tumor microenvironment and myeloid-derived suppressor cells. Cancer Microenviron, 2013. **6**(2): p. 169-77.

24. Katou, F., et al., Differing phenotypes between intraepithelial and stromal lymphocytes in early-stage tongue cancer. Cancer Res, 2007. **67**(23): p. 11195-201.

25. Kim, J. and J.S. Bae, Tumor-Associated Macrophages and Neutrophils in Tumor Microenvironment. Mediators Inflamm, 2016. **2016**: p. 6058147.

26. Nirmal, A.J., et al., Immune Cell Gene Signatures for Profiling the Microenvironment of Solid Tumors. Cancer Immunol Res, 2018. **6**(11): p. 1388-1400.

27. Peltanova, B., M. Raudenska, and M. Masarik, Effect of tumor microenvironment on pathogenesis of the head and neck squamous cell carcinoma: a systematic review. Mol Cancer, 2019. **18**(1): p. 63.

28. Mandal, R., et al., The head and neck cancer immune landscape and its immunotherapeutic implications. JCI Insight, 2016. **1**(17): p. e89829.

29. Garaud, S., et al., Tumor infiltrating B-cells signal functional humoral immune responses in breast cancer. JCI Insight, 2019. **5**(18).

30. Petitprez, F., et al., B cells are associated with survival and immunotherapy response in sarcoma. Nature, 2020. **577**(7791): p. 556-560.

31. Ruffin, A.T., et al., B cell signatures and tertiary lymphoid structures contribute to outcome in head and neck squamous cell carcinoma. Nat Commun, 2021. **12**(1): p. 3349.

32. Liang, B., Y. Tao, and T. Wang, Profiles of immune cell infiltration in head and neck squamous carcinoma. Biosci Rep, 2020. **40**(2).

33. Nagarsheth, N., M.S. Wicha, and W. Zou, Chemokines in the cancer microenvironment and their relevance in cancer immunotherapy. Nat Rev Immunol, 2017. **17**(9): p. 559-572.

34. Chow, M.T. and A.D. Luster, Chemokines in cancer. Cancer Immunol Res, 2014. **2**(12): p. 1125-31.

35. Ozga, A.J., M.T. Chow, and A.D. Luster, Chemokines and the immune response to cancer. Immunity, 2021. **54**(5): p. 859-874.

36. Korbecki, J., et al., CC Chemokines in a Tumor: A Review of Pro-Cancer and Anti-Cancer Properties of Receptors CCR5, CCR6, CCR7, CCR8, CCR9, and CCR10 Ligands. Int J Mol Sci, 2020. **21**(20).

37. Sica, A., P. Allavena, and A. Mantovani, Cancer related inflammation: the macrophage connection. Cancer Lett, 2008. **267**(2): p. 204-15.

38. Tokunaga, R., et al., CXCL9, CXCL10, CXCL11/CXCR3 axis for immune activation - A target for novel cancer therapy. Cancer Treat Rev, 2018. **63**: p. 40-47.

39. Yamashita, U. and E. Kuroda, Regulation of macrophage-derived chemokine (MDC, CCL22) production. Crit Rev Immunol, 2002. **22**(2): p. 105-14.

40. Anz, D., et al., Suppression of intratumoral CCL22 by type i interferon inhibits migration of regulatory T cells and blocks cancer progression. Cancer Res, 2015. **75**(21): p. 4483-93.

41. Mantovani, A., et al., Macrophage-derived chemokine (MDC). J Leukoc Biol, 2000. **68**(3): p. 400-4.

42. Vulcano, M., et al., Dendritic cells as a major source of macrophage-derived chemokine/CCL22 in vitro and in vivo. Eur J Immunol, 2001. **31**(3): p. 812-22.

43. Guan, H., et al., A brief perspective of drug resistance toward EGFR inhibitors: the crystal structures of EGFRs and their variants. Future Med Chem, 2017. **9**(7): p. 693-704.

44. Shan, Y., et al., Oncogenic mutations counteract intrinsic disorder in the EGFR kinase and promote receptor dimerization. Cell, 2012. **149**(4): p. 860-70.

45. Ayati, A., et al., Thiazole in the targeted anticancer drug discovery. Future Med Chem, 2019. **11**(15): p. 1929-1952.

46. Sharma, S.V., et al., Epidermal growth factor receptor mutations in lung cancer. Nat Rev Cancer, 2007. **7**(3): p. 169-81.

47. Alaoui-Jamali, M.A., G.B. Morand, and S.D. da Silva, ErbB polymorphisms: insights and implications for response to targeted cancer therapeutics. Front Genet, 2015. **6**: p. 17.

48. Yarden, Y. and G. Pines, The ERBB network: at last, cancer therapy meets systems biology. Nat Rev Cancer, 2012. **12**(8): p. 553-63.

49. Roskoski, R., Jr., The ErbB/HER family of protein-tyrosine kinases and cancer. Pharmacol Res, 2014. **79**: p. 34-74.

50. Arteaga, C.L. and J.A. Engelman, ERBB receptors: from oncogene discovery to basic science to mechanism-based cancer therapeutics. Cancer Cell, 2014. **25**(3): p. 282-303.

51. Paez, J.G., et al., EGFR mutations in lung cancer: correlation with clinical response to gefitinib therapy. Science, 2004. **304**(5676): p. 1497-500.

52. Slamon, D.J., et al., Use of chemotherapy plus a monoclonal antibody against HER2 for metastatic breast cancer that overexpresses HER2. N Engl J Med, 2001. **344**(11): p. 783-92.

53. Modi, S., et al., Trastuzumab Deruxtecan in Previously Treated HER2-Positive Breast Cancer. N Engl J Med, 2020. **382**(7): p. 610-621.

54. Ayati, A., et al., A review on progression of epidermal growth factor receptor (EGFR) inhibitors as an efficient approach in cancer targeted therapy. Bioorg Chem, 2020. **99**: p. 103811.

55. Le, T. and D.E. Gerber, Newer-Generation EGFR Inhibitors in Lung Cancer: How Are They Best Used? Cancers (Basel), 2019. **11**(3).

56. Bhartiya, D. and J. Singh, FSH-FSHR3-stem cells in ovary surface epithelium: basis for adult ovarian biology, failure, aging, and cancer. Reproduction, 2015. **149**(1): p. R35-48.

57. Rao, A. and D.R. Herr, G protein-coupled receptor GPR19 regulates E-cadherin expression and invasion of breast cancer cells. Biochim Biophys Acta Mol Cell Res, 2017. **1864**(7): p. 1318-1327.

58. Bang, Y.J., et al., Increased MAPK activity and MKP-1 overexpression in human gastric adenocarcinoma. Biochem Biophys Res Commun, 1998. **250**(1): p. 43-7.

59. Eblen, S.T., Extracellular-Regulated Kinases: Signaling From Ras to ERK Substrates to Control Biological Outcomes. Adv Cancer Res, 2018. **138**: p. 99-142.

60. O'Neill, E. and W. Kolch, Conferring specificity on the ubiquitous Raf/MEK signalling pathway. Br J Cancer, 2004. **90**(2): p. 283-8.

61. Sebolt-Leopold, J.S., et al., Blockade of the MAP kinase pathway suppresses growth of colon tumors in vivo. Nat Med, 1999. **5**(7): p. 810-6.

62. Sugiura, R., R. Satoh, and T. Takasaki, ERK: A Double-Edged Sword in Cancer. ERK-Dependent Apoptosis as a Potential Therapeutic Strategy for Cancer. Cells, 2021. **10**(10).

63. Revathidevi, S. and A.K. Munirajan, Akt in cancer: Mediator and more. Semin Cancer Biol, 2019. **59**: p. 80-91.

64. Noorolyai, S., et al., The relation between PI3K/AKT signalling pathway and cancer. Gene, 2019. **698**: p. 120-128.

65. Liu, H.W., et al., Satb1 promotes Schwann cell viability and migration via activation of PI3K/AKT pathway. Eur Rev Med Pharmacol Sci, 2018. **22**(13): p. 4268-4277.

66. Bellacosa, A., et al., Activation of AKT kinases in cancer: implications for therapeutic targeting. Adv Cancer Res, 2005. **94**: p. 29-86.

67. Ward, S.G., J. Westwick, and S. Harris, Sat-Nav for T cells: Role of PI3K isoforms and lipid phosphatases in migration of T lymphocytes. Immunol Lett, 2011. **138**(1): p. 15-8.

68. Wang, Z. and P.A. Cole, Catalytic mechanisms and regulation of protein kinases. Methods Enzymol, 2014. **548**: p. 1-21.

69. Drake, J.M., J.K. Lee, and O.N. Witte, Clinical targeting of mutated and wild-type protein tyrosine kinases in cancer. Mol Cell Biol, 2014. **34**(10): p. 1722-32.

70. Knösel, T., et al., [Tyrosine kinases in soft tissue tumors]. Pathologe, 2014. **35 Suppl 2**: p. 198-201.

71. Winkler, G.C., et al., Functional differentiation of cytotoxic cancer drugs and targeted cancer therapeutics. Regul Toxicol Pharmacol, 2014. **70**(1): p. 46-53.

72. De Silva, N., et al., Molecular effects of Lapatinib in the treatment of HER2 overexpressing oesophago-gastric adenocarcinoma. Br J Cancer, 2015. **113**(9): p. 1305-12.

73. Voigtlaender, M., T. Schneider-Merck, and M. Trepel, Lapatinib. Recent Results Cancer Res, 2018. **211**: p. 19-44.

74. Hsiao, Y.C., et al., Lapatinib increases motility of triple-negative breast cancer cells by decreasing miRNA-7 and inducing Raf-1/MAPK-dependent interleukin-6. Oncotarget, 2015. **6**(35): p. 37965-78.

75. Long, X.H., et al., Lapatinib alters the malignant phenotype of osteosarcoma cells via downregulation of the activity of the HER2-PI3K/AKT-FASN axis in vitro. Oncol Rep, 2014. **31**(1): p. 328-34.

76. Hicks, M., et al., Neoadjuvant dual HER2-targeted therapy with lapatinib and trastuzumab improves pathologic complete response in patients with early stage HER2-positive breast cancer: a meta-analysis of randomized prospective clinical trials. Oncologist, 2015. **20**(4): p. 337-43.

77. Bao, K., et al., Pharmacoeconomic Evaluation of Erlotinib for the Treatment of Pancreatic Cancer. Clin Ther, 2021. **43**(6): p. 1107-1115.

78. Zhang, Y., et al., Erlotinib enhanced chemoradiotherapy sensitivity via inhibiting DNA damage repair in nasopharyngeal carcinoma CNE2 cells. Ann Palliat Med, 2020. **9**(5): p. 2559-2567.

79. Lynch, T.J., et al., Activating mutations in the epidermal growth factor receptor underlying responsiveness of non-small-cell lung cancer to gefitinib. N Engl J Med, 2004. **350**(21): p. 2129-39.

80. Dumbrava, M.G., et al., Transforming growth factor beta signaling functions during mammalian kidney development. Pediatric Nephrology, 2021. **36**(7): p. 1663-1672.

81. Prud'homme, G.J., Pathobiology of transforming growth factor β in cancer, fibrosis and immunologic disease, and therapeutic considerations. Laboratory Investigation, 2007. **87**(11): p. 1077-1091.

82. Shi, Y. and J. Massagué, Mechanisms of TGF-beta signaling from cell membrane to the nucleus. Cell, 2003. **113**(6): p. 685-700.

83. Blobe, G.C., et al., Functional roles for the cytoplasmic domain of the type III transforming growth factor beta receptor in regulating transforming growth factor beta signaling. J Biol Chem, 2001. **276**(27): p. 24627-37.

84. Villarreal, M.M., et al., Binding Properties of the Transforming Growth Factor-β Coreceptor Betaglycan: Proposed Mechanism for Potentiation of Receptor Complex Assembly and Signaling. Biochemistry, 2016. **55**(49): p. 6880-6896.

85. Massagué, J., TGFβ in Cancer. Cell, 2008. **134**(2): p. 215-230.

86. Zhang, L., F. Zhou, and P. ten Dijke, Signaling interplay between transforming growth factor-β receptor and PI3K/AKT pathways in cancer. Trends in Biochemical Sciences, 2013. **38**(12): p. 612-620.

87. Sundqvist, A., P. Ten Dijke, and H. van Dam, Key signaling nodes in mammary gland development and cancer: Smad signal integration in epithelial cell plasticity. Breast Cancer Res, 2012. **14**(1): p. 204.

88. Bakin, A.V., et al., p38 mitogen-activated protein kinase is required for TGFbeta-mediated fibroblastic transdifferentiation and cell migration. J Cell Sci, 2002. **115**(Pt 15): p. 3193-206.

89. Bakin, A.V., et al., Phosphatidylinositol 3-kinase function is required for transforming growth factor beta-mediated epithelial to mesenchymal transition and cell migration. J Biol Chem, 2000. **275**(47): p. 36803-10.

90. Yu, L., M.C. Hébert, and Y.E. Zhang, TGF-beta receptor-activated p38 MAP kinase mediates Smad-independent TGF-beta responses. Embo j, 2002. **21**(14): p. 3749-59.

91. Stratton, M.R., P.J. Campbell, and P.A. Futreal, The cancer genome. Nature, 2009. **458**(7239): p. 719-24.

92. Podlaha, O., et al., Evolution of the cancer genome. Trends Genet, 2012. **28**(4): p. 155-63.

93. Matsushita, H., et al., Cancer exome analysis reveals a T-cell-dependent mechanism of cancer immunoediting. Nature, 2012. **482**(7385): p. 400-4.

94. Schreiber, R.D., L.J. Old, and M.J. Smyth, Cancer immunoediting: integrating immunity's roles in cancer suppression and promotion. Science, 2011. **331**(6024): p. 1565-70.

95. Vesely, M.D., et al., Natural innate and adaptive immunity to cancer. Annu Rev Immunol, 2011. **29**: p. 235-71.

96. Grivennikov, S.I., F.R. Greten, and M. Karin, Immunity, inflammation, and cancer. Cell, 2010. **140**(6): p. 883-99.

97. Seager, R.J., et al., Dynamic interplay between tumour, stroma and immune system can drive or prevent tumour progression. Converg Sci Phys Oncol, 2017. **3**.

98. Demaria, O., et al., Harnessing innate immunity in cancer therapy. Nature, 2019. **574**(7776): p. 45-56.

99. Yuen, G.J., E. Demissie, and S. Pillai, B lymphocytes and cancer: a love-hate relationship. Trends Cancer, 2016. **2**(12): p. 747-757.

100. Yang, Y., Cancer immunotherapy: harnessing the immune system to battle cancer. J Clin Invest, 2015. **125**(9): p. 3335-7.

101. Bremnes, R.M., et al., The Role of Tumor-Infiltrating Lymphocytes in Development, Progression, and Prognosis of Non-Small Cell Lung Cancer. J Thorac Oncol, 2016. **11**(6): p. 789-800.

102. Tuminello, S., et al., Prognostic value of immune cells in the tumor microenvironment of early-stage lung cancer: a meta-analysis. Oncotarget, 2019. **10**(67): p. 7142-7155.

103. Hanahan, D. and R.A. Weinberg, Hallmarks of cancer: the next generation. Cell, 2011. **144**(5): p. 646-74.

104. Dhatchinamoorthy, K., J.D. Colbert, and K.L. Rock, Cancer Immune Evasion Through Loss of MHC Class I Antigen Presentation. Front Immunol, 2021. **12**: p. 636568.

105. de la Iglesia, J.V., et al., Effects of Tobacco Smoking on the Tumor Immune Microenvironment in Head and Neck Squamous Cell Carcinoma. Clin Cancer Res, 2020. **26**(6): p. 1474-1485.

106. Ferris, R.L., Immunology and Immunotherapy of Head and Neck Cancer. J Clin Oncol, 2015. **33**(29): p. 3293-304.

107. Wondergem, N.E., et al., The Immune Microenvironment in Head and Neck Squamous Cell Carcinoma: on Subsets and Subsites. Curr Oncol Rep, 2020. **22**(8): p. 81.

108. Saada-Bouzid, E., F. Peyrade, and J. Guigay, Immunotherapy in recurrent and or metastatic squamous cell carcinoma of the head and neck. Curr Opin Oncol, 2019. **31**(3): p. 146-151.

109. Khong, H.T. and N.P. Restifo, Natural selection of tumor variants in the generation of "tumor escape" phenotypes. Nat Immunol, 2002. **3**(11): p. 999-1005.

110. Bubeník, J., MHC class I down-regulation: tumour escape from immune surveillance? (review). Int J Oncol, 2004. **25**(2): p. 487-91.

111. Ogino, T., et al., HLA class I antigen down-regulation in primary laryngeal squamous cell carcinoma lesions as a poor prognostic marker. Cancer Res, 2006. **66**(18): p. 9281-9.

112. Oliva, M., et al., Immune biomarkers of response to immune-checkpoint inhibitors in head and neck squamous cell carcinoma. Ann Oncol, 2019. **30**(1): p. 57-67.

113. Hanna, G.J., et al., Frameshift events predict anti-PD-1/L1 response in head and neck cancer. JCI Insight, 2018. **3**(4).

114. Gao, A., et al., Predictive factors in the treatment of oral squamous cell carcinoma using PD-1/PD-L1 inhibitors. Invest New Drugs, 2021. **39**(4): p. 1132-1138.

115. Cornel, A.M., I.L. Mimpen, and S. Nierkens, MHC Class I Downregulation in Cancer: Underlying Mechanisms and Potential Targets for Cancer Immunotherapy. Cancers (Basel), 2020. **12**(7).

116. Diedrich, G., et al., A role for calnexin in the assembly of the MHC class I loading complex in the endoplasmic reticulum. J Immunol, 2001. **166**(3): p. 1703-9.

117. Rock, K.L., E. Reits, and J. Neefjes, Present Yourself! By MHC Class I and MHC Class II Molecules. Trends Immunol, 2016. **37**(11): p. 724-737.

118. Kotsias, F., I. Cebrian, and A. Alloatti, Antigen processing and presentation. Int Rev Cell Mol Biol, 2019. **348**: p. 69-121.

119. Reeves, E. and E. James, Antigen processing and immune regulation in the response to tumours. Immunology, 2017. **150**(1): p. 16-24.

120. Takahashi, A., et al., Tyrosine Kinase Inhibitors Stimulate HLA Class I Expression by Augmenting the IFNγ/STAT1 Signaling in Hepatocellular Carcinoma Cells. Front Oncol, 2021. **11**: p. 707473.

121. Watanabe, S., et al., Mutational activation of the epidermal growth factor receptor down-regulates major histocompatibility complex class I expression via the extracellular signal-regulated kinase in non-small cell lung cancer. Cancer Sci, 2019. **110**(1): p. 52-60.

122. Brea, E.J., et al., Kinase Regulation of Human MHC Class I Molecule Expression on Cancer Cells. Cancer Immunol Res, 2016. **4**(11): p. 936-947.

123. Ebert, P.J.R., et al., MAP Kinase Inhibition Promotes T Cell and Anti-tumor Activity in Combination with PD-L1 Checkpoint Blockade. Immunity, 2016. **44**(3): p. 609-621.

124. Sapkota, B., C.E. Hill, and B.P. Pollack, Vemurafenib enhances MHC induction in BRAF(V600E) homozygous melanoma cells. Oncoimmunology, 2013. **2**(1): p. e22890.

125. Schrörs, B., et al., HLA class I loss in metachronous metastases prevents continuous T cell recognition of mutated neoantigens in a human melanoma model. Oncotarget, 2017. **8**(17): p. 28312-28327.

126. Romero, I., et al., MHC Intratumoral Heterogeneity May Predict Cancer Progression and Response to Immunotherapy. Front Immunol, 2018. **9**: p. 102.

127. del Campo, A.B., et al., Immune escape of cancer cells with beta2-microglobulin loss over the course of metastatic melanoma. Int J Cancer, 2014. **134**(1): p. 102-13.

128. Erdogdu, I.H., MHC Class 1 and PDL-1 Status of Primary Tumor and Lymph Node Metastatic Tumor Tissue in Gastric Cancers. Gastroenterol Res Pract, 2019. **2019**: p. 4785098.

129. Zhang, N. and M.J. Bevan, CD8(+) T cells: foot soldiers of the immune system. Immunity, 2011. **35**(2): p. 161-8.

130. Francisco, L.M., P.T. Sage, and A.H. Sharpe, The PD-1 pathway in tolerance and autoimmunity. Immunol Rev, 2010. **236**: p. 219-42.

131. Freeman, G.J., et al., Engagement of the PD-1 immunoinhibitory receptor by a novel B7 family member leads to negative regulation of lymphocyte activation. J Exp Med, 2000. **192**(7): p. 1027-34.

132. Dong, H., et al., Tumor-associated B7-H1 promotes T-cell apoptosis: a potential mechanism of immune evasion. Nat Med, 2002. **8**(8): p. 793-800.

133. Du, S., et al., Blockade of Tumor-Expressed PD-1 promotes lung cancer growth. Oncoimmunology, 2018. **7**(4): p. e1408747.

134. He, R., et al., PD-1 Expression in Chronic Lymphocytic Leukemia/Small Lymphocytic Lymphoma (CLL/SLL) and Large B-cell Richter Transformation (DLBCL-RT): A Characteristic Feature of DLBCL-RT and Potential Surrogate Marker for Clonal Relatedness. Am J Surg Pathol, 2018. **42**(7): p. 843-854.

135. Yao, H., et al., Cancer Cell-Intrinsic PD-1 and Implications in Combinatorial Immunotherapy. Front Immunol, 2018. **9**: p. 1774.

136. Thompson, R.H., et al., Costimulatory B7-H1 in renal cell carcinoma patients: Indicator of tumor aggressiveness and potential therapeutic target. Proc Natl Acad Sci U S A, 2004. **101**(49): p. 17174-9.

137. Ohaegbulam, K.C., et al., Human cancer immunotherapy with antibodies to the PD-1 and PD-L1 pathway. Trends Mol Med, 2015. **21**(1): p. 24-33.

138. Ni, J.M. and A.P. Ni, Landscape of PD-1/PD-L1 Regulation and Targeted Immunotherapy. Chin Med Sci J, 2018. **33**(3): p. 174-182.

139. Jiang, X., et al., The activation of MAPK in melanoma cells resistant to BRAF inhibition promotes PD-L1 expression that is reversible by MEK and PI3K inhibition. Clin Cancer Res, 2013. **19**(3): p. 598-609.

140. Qin, X., et al., Cisplatin induces programmed death-1-ligand 1(PD-L1) over-expression in hepatoma H22 cells via Erk /MAPK signaling pathway. Cell Mol Biol (Noisy-le-grand), 2010. **56 Suppl**: p. Ol1366-72.

141. Coelho, M.A., et al., Oncogenic RAS Signaling Promotes Tumor Immunoresistance by Stabilizing PD-L1 mRNA. Immunity, 2017. **47**(6): p. 1083-1099.e6.

142. Shi, J., et al., Human immunodeficiency virus type 1 Tat induces B7-H1 expression via ERK/MAPK signaling pathway. Cell Immunol, 2011. **271**(2): p. 280-5.

143. Song, M., et al., PTEN loss increases PD-L1 protein expression and affects the correlation between PD-L1 expression and clinical parameters in colorectal cancer. PLoS One, 2013. **8**(6): p. e65821.

144. Crane, C.A., et al., PI(3) kinase is associated with a mechanism of immunoresistance in breast and prostate cancer. Oncogene, 2009. **28**(2): p. 306-12.

145. Parsa, A.T., et al., Loss of tumor suppressor PTEN function increases B7-H1 expression and immunoresistance in glioma. Nat Med, 2007. **13**(1): p. 84-8.

146. Lastwika, K.J., et al., Control of PD-L1 Expression by Oncogenic Activation of the AKT-mTOR Pathway in Non-Small Cell Lung Cancer. Cancer Res, 2016. **76**(2): p. 227-38.

147. Sever, R. and J.S. Brugge, Signal transduction in cancer. Cold Spring Harb Perspect Med, 2015. **5**(4).

148. Seliger, B., et al., Immune Escape Mechanisms and Their Clinical Relevance in Head and Neck Squamous Cell Carcinoma. Int J Mol Sci, 2020. **21**(19).

149. Brand, T.M., M. Iida, and D.L. Wheeler, Molecular mechanisms of resistance to the EGFR monoclonal antibody cetuximab. Cancer Biol Ther, 2011. **11**(9): p. 777-92.

150. Hammoud, M.K., et al., Raman micro-spectroscopy monitors acquired resistance to targeted cancer therapy at the cellular level. Scientific Reports, 2018. **8**(1): p. 15278.

151. Zhang, M., et al., TGF-β Signaling and Resistance to Cancer Therapy. Front Cell Dev Biol, 2021. **9**: p. 786728.

152. Long, Z., J.R. Grandis, and D.E. Johnson, Emerging tyrosine kinase inhibitors for head and neck cancer. Expert Opin Emerg Drugs, 2022. **27**(3): p. 333-344.

153. Martinez-Useros, J. and J. Garcia-Foncillas, The challenge of blocking a wider family members of EGFR against head and neck squamous cell carcinomas. Oral Oncol, 2015. **51**(5): p. 423-30.

154. Horton, J.D., et al., Immune Evasion by Head and Neck Cancer: Foundations for Combination Therapy. Trends Cancer, 2019. **5**(4): p. 208-232.

155. Blume-Jensen, P. and T. Hunter, Oncogenic kinase signalling. Nature, 2001. **411**(6835): p. 355-65.

156. Annenkov, A., Receptor tyrosine kinase (RTK) signalling in the control of neural stem and progenitor cell (NSPC) development. Mol Neurobiol, 2014. **49**(1): p. 440-71.

157. Butti, R., et al., Receptor tyrosine kinases (RTKs) in breast cancer: signaling, therapeutic implications and challenges. Mol Cancer, 2018. **17**(1): p. 34.

158. De Pauw, I., et al., Simultaneous targeting of EGFR, HER2, and HER4 by afatinib overcomes intrinsic and acquired cetuximab resistance in head and neck squamous cell carcinoma cell lines. Mol Oncol, 2018. **12**(6): p. 830-854.

159. de Souza, J.A., et al., A phase II study of lapatinib in recurrent/metastatic squamous cell carcinoma of the head and neck. Clin Cancer Res, 2012. **18**(8): p. 2336-43.

160. Harrington, K., et al., Postoperative Adjuvant Lapatinib and Concurrent Chemoradiotherapy Followed by Maintenance Lapatinib Monotherapy in High-Risk Patients With Resected Squamous Cell Carcinoma of the Head and Neck: A Phase III, Randomized, Double-Blind, Placebo-Controlled Study. J Clin Oncol, 2015. **33**(35): p. 4202-9.

161. Rosenthal, E.L., et al., Assessment of erlotinib as adjuvant chemoprevention in high-risk head and neck cancer patients. Ann Surg Oncol, 2014. **21**(13): p. 4263-9.

162. Soulieres, D., et al., Multicenter phase II study of erlotinib, an oral epidermal growth factor receptor tyrosine kinase inhibitor, in patients with recurrent or metastatic squamous cell cancer of the head and neck. J Clin Oncol, 2004. **22**(1): p. 77-85.

163. Dyckhoff, G., et al., Human Leucocyte Antigens as Prognostic Markers in Head and Neck Squamous Cell Carcinoma. Cancers (Basel), 2022. **14**(15).

164. Jongsma, M.L.M., G. Guarda, and R.M. Spaapen, The regulatory network behind MHC class I expression. Molecular Immunology, 2019. **113**: p. 16-21.

165. Garrido, F., HLA Class-I Expression and Cancer Immunotherapy. Adv Exp Med Biol, 2019. **1151**: p. 79-90.

166. Aptsiauri, N., F. Ruiz-Cabello, and F. Garrido, The transition from HLA-I positive to HLA-I negative primary tumors: the road to escape from T-cell responses. Curr Opin Immunol, 2018. **51**: p. 123-132.

167. Boegel, S., et al., HLA and proteasome expression body map. BMC Med Genomics, 2018. **11**(1): p. 36.

168. Uhlen, M., et al., A genome-wide transcriptomic analysis of protein-coding genes in human blood cells. Science, 2019. **366**(6472).

169. Garrido, F., MHC/HLA Class I Loss in Cancer Cells. Adv Exp Med Biol, 2019. **1151**: p. 15-78.

170. Aptsiauri, N., et al., Role of altered expression of HLA class I molecules in cancer progression. Adv Exp Med Biol, 2007. **601**: p. 123-31.

171. Garrido, F., et al., Generation of MHC class I diversity in primary tumors and selection of the malignant phenotype. Int J Cancer, 2016. **138**(2): p. 271-80.

172. Chaganty, B.K., et al., Trastuzumab upregulates expression of HLA-ABC and T cell costimulatory molecules through engagement of natural killer cells and stimulation of IFNγ secretion. Oncoimmunology, 2016. **5**(4): p. e1100790.

173. Gou, Q., et al., PD-L1 degradation pathway and immunotherapy for cancer. Cell Death Dis, 2020. **11**(11): p. 955.

174. Sun, C., R. Mezzadra, and T.N. Schumacher, Regulation and Function of the PD-L1 Checkpoint. Immunity, 2018. **48**(3): p. 434-452.

175. Cha, J.H., et al., Mechanisms Controlling PD-L1 Expression in Cancer. Mol Cell, 2019. **76**(3): p. 359-370.

176. Bindea, G., et al., Spatiotemporal dynamics of intratumoral immune cells reveal the immune landscape in human cancer. Immunity, 2013. **39**(4): p. 782-95.

177. Fridman, W.H., et al., The immune contexture in cancer prognosis and treatment. Nat Rev Clin Oncol, 2017. **14**(12): p. 717-734.

178. Gentles, A.J., et al., The prognostic landscape of genes and infiltrating immune cells across human cancers. Nat Med, 2015. **21**(8): p. 938-945.

179. Ruffell, B. and L.M. Coussens, Macrophages and therapeutic resistance in cancer. Cancer Cell, 2015. **27**(4): p. 462-72.

180. Josephs, D.H., H.J. Bax, and S.N. Karagiannis, Tumour-associated macrophage polarisation and re-education with immunotherapy. FBE, 2015. **7**(2): p. 334-351.

181. Xavier, F.C.A., et al., Mechanisms of immune evasion by head and neck cancer stem cells. Front Oral Health, 2022. **3**: p. 957310.

182. Chen, Y., et al., An Immune-Related Gene Prognostic Index for Head and Neck Squamous Cell Carcinoma. Clin Cancer Res, 2021. **27**(1): p. 330-341.

183. Batlle, E. and J. Massagué, Transforming Growth Factor-β Signaling in Immunity and Cancer. Immunity, 2019. **50**(4): p. 924-940.

184. Chang, A.L., et al., CCL2 Produced by the Glioma Microenvironment Is Essential for the Recruitment of Regulatory T Cells and Myeloid-Derived Suppressor Cells. Cancer Res, 2016. **76**(19): p. 5671-5682.

185. Cook, K.W., et al., CCL20/CCR6-mediated migration of regulatory T cells to the Helicobacter pylori-infected human gastric mucosa. Gut, 2014. **63**(10): p. 1550-9.

186. Osuala, K.O. and B.F. Sloane, Many Roles of CCL20: Emphasis on Breast Cancer. Postdoc J, 2014. **2**(3): p. 7-16.

187. Sugiyama, E., et al., Blockade of EGFR improves responsiveness to PD-1 blockade in EGFR-mutated non-small cell lung cancer. Sci Immunol, 2020. **5**(43).

188. Harlin, H., et al., Chemokine expression in melanoma metastases associated with CD8+ T-cell recruitment. Cancer Res, 2009. **69**(7): p. 3077-85.

189. Dangaj, D., et al., Cooperation between Constitutive and Inducible Chemokines Enables T Cell Engraftment and Immune Attack in Solid Tumors. Cancer Cell, 2019. **35**(6): p. 885-900.e10.

190. Böttcher, J.P., et al., NK Cells Stimulate Recruitment of cDC1 into the Tumor Microenvironment Promoting Cancer Immune Control. Cell, 2018. **172**(5): p. 1022-1037.e14.

8 Theses

1. Lapatinib and erlotinib, EGFR inhibitors, effectively suppress tumor development in head and neck squamous cell carcinoma (HNSCC) cells by inhibiting EGFR phosphorylation. Lapatinib shows superior inhibition of AKT and ERK phosphorylation, particularly in PCI-4B cells.

2. Multiple signaling pathways, including EGFR-related pathways, regulate AKT and ERK activation in HNSCC. Upregulated TGFβ and its receptors activate EGFR-dependent AKT and ERK signaling, highlighting the potential of Tyrosine kinase inhibitors (TKIs) and TGFβ inhibitors for HNSCC treatment.

3. EGFR inhibitors reduce the expression of PD-L1, potentially enhancing anti-tumor immunity, while also upregulating HLA-ABC expression, promoting immune recognition against HNSCC.

4. The response of primary and metastatic HNSCC cell lines to lapatinib and erlotinib is generally consistent, with some variations in specific components that require further investigation.

5. Immunostaining analyses of clinical HNSCC patient sections reveal differences in immune cells between primary and metastatic tumor samples, emphasizing the importance of personalized treatment approaches.

6. TKI treatment affects immune-related factors and chemokines, supporting the potential of immunotherapy as a treatment option for HNSCC.

7. The multi-faceted response of HNSCC cell lines to TKIs, mediated through multiple signaling pathways, highlights the promise of combination therapy, including immunotherapy, for HNSCC treatment.

Publications and Conference Presentations

1. Seliger B, Massa C, **Yang B**, Bethmann D, Kappler M, Eckert AW, Wickenhauser C. Immune Escape Mechanisms and Their Clinical Relevance in Head and Neck Squamous Cell Carcinoma. Int J Mol Sci. 2020 Sep 24;21(19):7032. doi: 10.3390/ijms21197032.

2. Seliger B, Al-Samadi A, **Yang B**, Salo T, Wickenhauser C. In vitro models as tools for screening treatment options of head and neck cancer. Front Med (Lausanne). 2022 Sep 7;9:971726. doi: 10.3389/fmed.2022.971726.

3. Seliger B, Jasinski-Bergner S, Massa C, Mueller A, Biehl K, **Yang B**, Bachmann M, Jonigk D, Eichhorn P, Hartmann A, Wickenhauser C, Bauer M. Induction of pulmonary HLA-G expression by SARS-CoV-2 infection. Cell Mol Life Sci. 2022 Nov 5;79(11):582. doi: 10.1007/s00018-022-04592-9.

4. **Yang B**, Wickenhauser C, Al-Samadi A, Seliger B. The function of lapatinib and erlotinib in EGFR-related pathways and their immune-modulatory effects in head and neck squamous carcinoma. Tumor Immunology meets Oncology XVI. 2022 July, Halle (Saale), Germany. (Poster)

Declarations

1. I declare that I have not completed or initiated a doctorate procedure at any other university.
2. I declare that all information given is accurate and complete. The thesis has not been used previously at this or any other university in order to achieve an academic degree.
3. I declare under oath that this thesis is my own work entirely and has been written without any help from other people. I met all regulations of good scientific practice and I used only the sources mentioned and included all the citations correctly both in word and in content.

Bo Yang

Halle (Saale), 02.04.2023

Acknowledgments

I have received great help and support during my whole studies.

First of all, I would like to thank Prof. Barbara Seliger and Prof. Claudia Wickenhauser for providing the topic and scientific advice during my PhD thesis.

I would also like to thank Dr. Chiara Massa, Dr. Karthik Subbaryan and Dr. Simon Jasinski-Bergner, postdocs at the Institute, for their patience in helping me to solve the problems I encountered during the experiments.

I also thank Ph.D. students Georgiana Toma, Ulagappan Kamatchi, Yuan Wang, Christoforos Vaxevanis, and Udinotti Mario for their help.

I would like to thank Ms. Anja Müller and Ms. Katharina Biehl for their technical support throughout the experimental process.

I would also like to thank Prof. Claudia Wickenhauser and Prof. Ahmed Al-Samadi for providing human tissue samples of HNSCC and the Pathology Institute of Halle University for providing the equipment and platform for immunoassays.

Also, I would like to thank Chiara Massa, Marcus Bauer, and Marius Wunderle for their patience in teaching me during the analysis of immunological results.

I would also like to thank Nicole Ott, Maria Heise and Lukas Mittag for their excellent secretarial work.

I express my gratitude to the China National Scholarship Council for providing financial support.

Finally, I would like to thank my family members for their understanding and support during my studies.